Design of the Psychrometric Calorimeter Chamber of a Room Air Conditioner Test Facility

J. E. Fleming and W. E. Dunn

ACRC TR-44 July 1993

For additional information:

Air Conditioning and Refrigeration Center
University of Illinois
Mechanical & Industrial Engineering Dept.
1206 West Green Street
Urbana, IL 61801

(217) 333-3115

Prepared as part of ACRC Project 23
Room Air Conditioner Systems Analysis
W. E. Dunn, Principal Investigator

The Air Conditioning and Refrigeration Center was founded in 1988 with a grant from the estate of Richard W. Kritzer, the founder of Peerless of America Inc. A State of Illinois Technology Challenge Grant helped build the laboratory facilities. The ACRC receives continuing support from the Richard W. Kritzer Endowment and the National Science Foundation. The following organizations have also become sponsors of the Center.

Acustar Division of Chrysler
Allied-Signal, Inc.
Amana Refrigeration, Inc.
Carrier Corporation
Caterpillar, Inc.
E. I. du Pont de Nemours & Co.
Electric Power Research Institute
Ford Motor Company
General Electric Company
Harrison Division of GM
ICI Americas, Inc.
Johnson Controls, Inc.
Modine Manufacturing Co.
Peerless of America, Inc.
Environmental Protection Agency
U. S. Army CERL
Whirlpool Corporation

For additional information:

Air Conditioning & Refrigeration Center
Mechanical & Industrial Engineering Dept.
University of Illinois
1206 West Green Street
Urbana IL 61801

217 333 3115

DESIGN OF THE PSYCHROMETRIC CALORIMETER CHAMBER OF A ROOM AIR CONDITIONER TEST FACILITY

Jonathan Edward Fleming, M.S.
Department of Mechanical and Industrial Engineering
University of Illinois at Urbana-Champaign, 1993
W. E. Dunn, Advisor

ABSTRACT

This report summarizes the process of designing the calorimeter chamber of a test facility for assessing the steady-state energy efficiency of room air conditioners. The calorimeter has been designed to produce accurate measurements of the cooling and dehumidifying abilities of room air conditioners rated between 0.5 and 2.5 tons of refrigeration. By designing the system to provide the air conditioners with a wide range of indoor psychrometric conditions, a rich data set can be obtained which will be used for determining the effects of alternative refrigerants and associated design changes on system performance.

Operating characteristics of the chamber have been identified and documented. Chamber performance data have quantified the parasitic steady-state heat and moisture losses which must be known in order to acquire accurate performance data. Transient testing of the facility has yielded the response characteristics of the system which are useful for optimal facility operation.

TABLE OF CONTENTS

LIST OF TABLES

LIST OF FIGURES

NOMENCLATURE

Symbols

A	total area of the walls of the indoor room
A_j	areas of the individual walls of the indoor room
d_w	mean diameter of screen wire
D_h	hydraulic diameter of rectangular duct
f	Moody friction factor, fraction of energy from reconditioning equiptment going into the air
L	length of rectangular duct
P	air pressure
Q_{in}	heat input into the indoor room
R_f	flow resistance coefficient
Re_w	Reynolds number based on wire diameter
T_j	temperature of the air spaces surrounding each of the walls of the indoor room
UA	overall heat transfer coefficient-area product for the indoor room
V_m	flow mean velocity
δ	ratio of screen open area to total area
μ	dynamic viscosity of air
ρ_g	density of air
T_a	average indoor room temperature
ω_a	average indoor room humidity ratio
m_a	mass of the air in the indoor room
c_{pa}	effective specific heat of the air in the indoor room
T_w	average wall temperature

m_w	mass of the walls
c_{pw}	effective specific heat if the walls
$\dot{Q}_R$	rate of thermal energy addition by reconditioning equiptment
$\dot{m}_R$	rate of moisture addition by reconditioning equiptment
$\dot{Q}_1$	rate at which the air and walls of the room exchange heat
U_1	overall heat transfer coefficient between the walls and air
A_1	contact area between the walls and air
T_{amb}	area-weighted average temperature of the ambient
$\dot{Q}_2$	rate of heat exchange to the ambient
U_2	overall heat transfer coefficient between the walls and the ambient
A_2	contact area between the walls and the ambient
U_m	effective mass transfer coefficient between the indoor and outdoor rooms
A_m	effective mass transfer area between the indoor and outdoor rooms
ω_{od}	average humidity ratio for the outdoor room
$\dot{Q}_T$	rate of heat removal by the test unit
$\dot{m}_T$	rate of moisture removal by the test unit
c_1, c_2 , c_3, c_4	constants used in the solution of the indoor room model
α_1, α_2, α_3, α_4	parameters used in the solution of the indoor room model
λ_1, λ_2, λ_3	eigenvalues used in the solution of the indoor room model

Acronyms

ASHRAE	American Society of Heating, Refrigerating, and Air-Condtioning Engineers

EER	Energy Efficiency Ratio = ratio of the heat removal rate of an air conditioner in Btu/hr to its power requirement in W

1. INTRODUCTION AND LITERATURE REVIEW

1.1 Motivation and Goals

Due to tightening of government mandated energy-efficiency standards on household appliances (NAECA 1987) as well as the commonly held belief that chlorofluorocarbons (CFCs) deplete the stratospheric ozone layer, there has been much interest in determining the energy performance implications of room air conditioner design changes and refrigerant substitution. The United Nations' Montreal Protocol defined a structure for the eventual elimination of ozone-depleting substances (United Nations 1987). The phaseout deadline for CFCs has been set for 1996 (Miro 1993) and, consequently, recent pressure to meet this deadline has been felt in CFC-related fields. The working fluid in room air conditioner systems is R22, a hydrochlorofluorocarbon (HCFC), which does not have as great an ozone-depletion potential as a CFC. Consequently, the phaseout schedule for the production and use of this compound is not as immediate as it is for CFCs. However, there is concern in the air-conditioning and refrigeration community about the possibility of increased pressure from either the EPA or the United Nations for quicker phaseout of HCFCs (ASHRAE 1993; Miro 1993). The search for alternative refrigerants for R22 coupled with governmental demand for higher-efficiency appliances has created a great need for performance evaluation.

The purpose of this paper is to (a) describe the process of designing the calorimeter chamber of a room air conditioner test facility, (b) describe the behavioral characteristics of the facility and (c) provide some validation of its utility. This design work has been conducted in order to produce accurate performance data for validating the Oak Ridge National Laboratory Heat Pump Model as modified for room air conditioners. Validation of this model or a derivative of the model for R22 and its alternatives will yield a product which can accurately simulate room air conditioner performance without the need for expensive and time-consuming testing. Throughout the development of model validation and/or modification, performance data will be used to determine the effects of design changes and alternative refrigerants on system performance.

1.2 Room Air Conditioner Test Facilities

The purpose of the test facility is to collect performance data on room air conditioners. As prescribed by the American Society of Heating Refrigerating and Air-

Conditioning Engineers (ASHRAE), these measurements are to include air-side data on (a) cooling capacity, (b) moisture removal capability and (c) air mass flow rates through each heat exchanger of the air conditioner (ASHRAE 1984). As well as these measurements, our facility will be equipped to make complementary refrigerant-side cooling measurements. However, the concern of this work is primarily with the air-side measurements specified by ASHRAE.

1.2.1 Air Conditioner Heat and Moisture Transfer Mechanisms

An important concern in the design of a room air conditioner test facility are the heat and mass transfer mechanisms of the air conditioner. For this reason, a discussion of the workings of a room air conditioner is warranted. Figure 1.1 shows a schematic of the top view of a typical room air conditioner. A compressor does work on low pressure R22 and raises the pressure and temperature of the gas to a level where the temperature is greater than outdoor temperature. This gas is then forced through a fin-and-tube condenser where it transfers heat to the outdoor air with help from an axial fan and thus becomes liquid or a two-phase mixture. This product is forced through a capillary-tube expansion device which lowers the temperature of the now two-phase refrigerant to a level which is below indoor temperature. The two-phase mixture is then forced through a fin-and-tube evaporator where it gains heat from the indoor air with help from a centrifugal fan and thus increases in quality or fully evaporates. The evaporator exit condition may be vapor, in which case it goes directly into the compressor to repeat the thermodynamic cycle. Otherwise, the liquid portion of the two-phase exit condition is separated from the bulk flow in an accumulator. As soon as the necessary heat for evaporation is transferred to the liquid by the gas or through the accumulator shell by the outdoor air, the refrigerant will rejoin the flow. The air conditioner has the capability to remove heat from the indoor room through heat transfer to the evaporator and can reject heat to the outdoor air through heat transfer from the condenser.

A more subtle attribute of the air conditioner is the ability to transfer moisture from the indoor air to the outdoor air. When the air conditioner is operating at an indoor room condition with a dew point temperature higher than the evaporator coil temperature, the coil condenses moisture out of the air which then drips into a collecting pan. From here, it flows downhill through a channel in the floor of the air conditioner until it reaches another collecting pan situated beneath the condenser fan in the outdoor space. This fan has a cupped ring, commonly known as a "slinger ring",

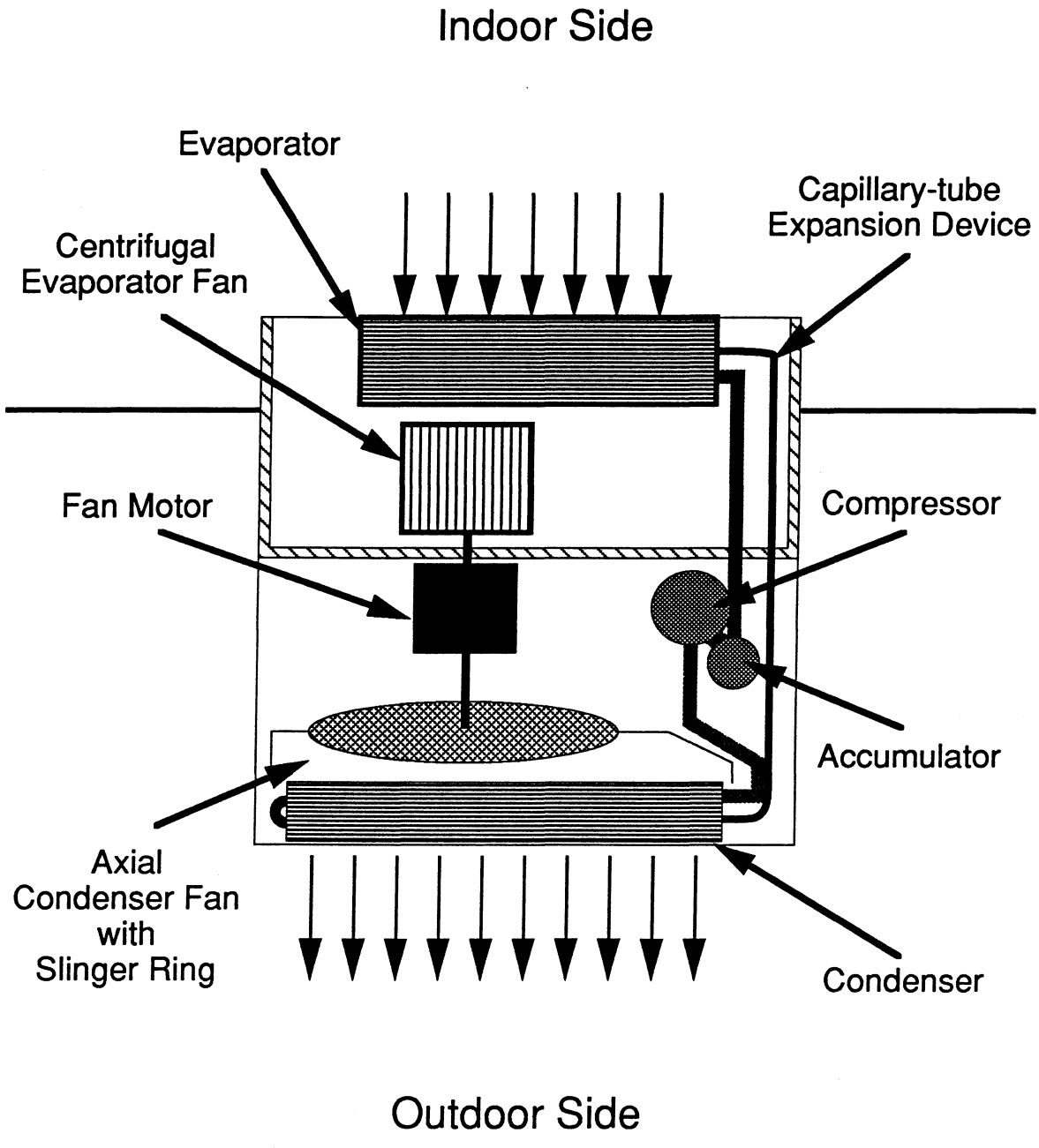

Figure 1.1 Room Air Conditioner Schematic

attached to the outer edge of the fan blades which lifts water out of the collecting pan and throws it on the fin-and-tube condenser. This water enhances heat transfer to the air by evaporating off the condenser which allows moisture transfer to occur between the indoor room and the outdoor room.

1.2.2 ASHRAE Standard Test Facilities

ASHRAE Standard 16-1983 describes two different test chamber scenarios. The first of these, called a calibrated room calorimeter, is shown in Figure 1.2. It consists of indoor and outdoor side compartments with a room air conditioner inserted into the wall partitioning the compartments. Each compartment is separately maintained at different but constant temperature and relative humidity. Since the air conditioner removes heat and moisture from the indoor room, these quantities must be replenished at the same rates in order to maintain a constant condition. A heater and humidifier, shown in Figure 1.2, are supplied for this reason. The reconditioned air in the indoor room must be mixed with the resident air to keep temperature and humidity stratification in the room to a minimum. Air movement in the room is provided by a fan which is required to circulate air at a rate at least twice that of the evaporator fan and no less than one room air change per minute. Airflow within three feet of the face of the air conditioner must have a velocity less than 100 fpm (ASHRAE 1984).

Heat and moisture are added to the outdoor side compartment by the room air conditioner and so they must be removed at the same rates in order to maintain a constant psychrometric condition in the room. For this reason, a cooling device and dehumidifier must be specified for the outdoor room. Again, the room air must be mixed to reduce stratification and the velocity requirement around the air conditioner is the same as in the indoor room. Also, the circulation of air in this room must be at least twice that of the condenser fan and no less than one outdoor room air change per minute (ASHRAE 1984).

The ASHRAE Standard Calorimeter uses a pressure equalizing device mounted in the wall partitioning the indoor and outdoor rooms. This device must alleviate any pressure difference between the two rooms by allowing air exchange through the partition wall. Airflow through the wall must be measured in order to determine the heat and moisture leakage in either direction (ASHRAE 1984).

The amount of cooling and dehumidification accomplished by the air conditioner is obtained by measuring the necessary heat and moisture added to the indoor room to maintain a steady-state temperature and humidity. ASHRAE specifies the walls of

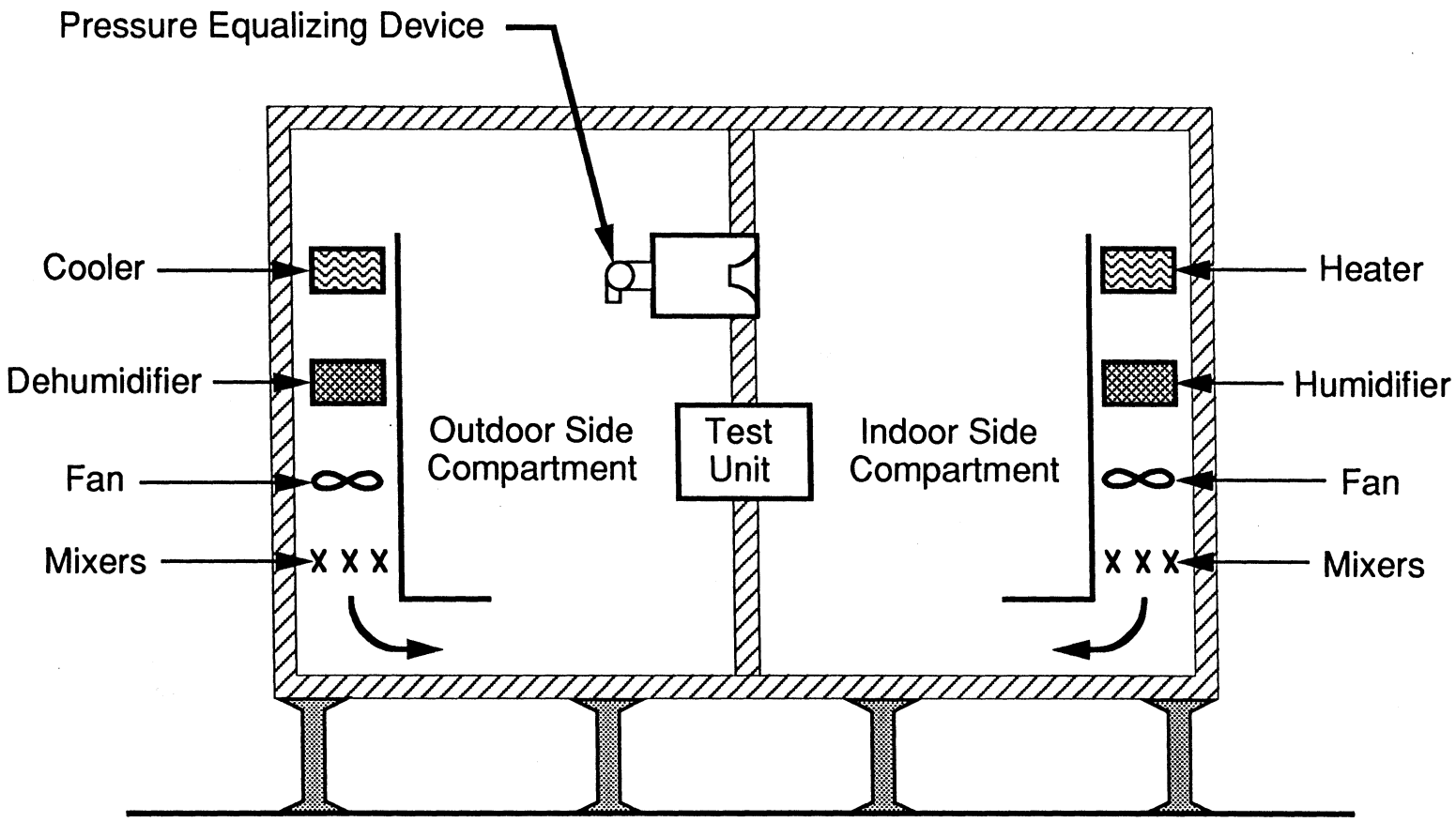

Figure 1.2 Calibrated Room Calorimeter

the chamber to be made of a non-porous material with all joints sealed to prevent air and moisture leakage. Since the chamber will be moisture-sealed, the dehumidification of the air conditioner can be quantified by measuring the amount of moisture added to the room. Heat loss from the chamber must be calibrated in order to determine the sensible cooling accomplished by the air conditioner. By measuring the heat added to the indoor room and adjusting this by the heat lost or gained through the walls, the sensible cooling will be determined (ASHRAE 1984).

The second chamber design described by ASHRAE and shown in Figure 1.3 is called the balanced ambient calorimeter. The only difference between this chamber and the previous one is the existence of a controlled-temperature air space around it. This air space is maintained at the same temperature as the indoor side compartment. In this manner, the only heat loss from the indoor room will be through the partition wall. This approach allows for a more reliable sensible cooling measurement since one need only calibrate the heat transfer between the two compartments(ASHRAE 1984).

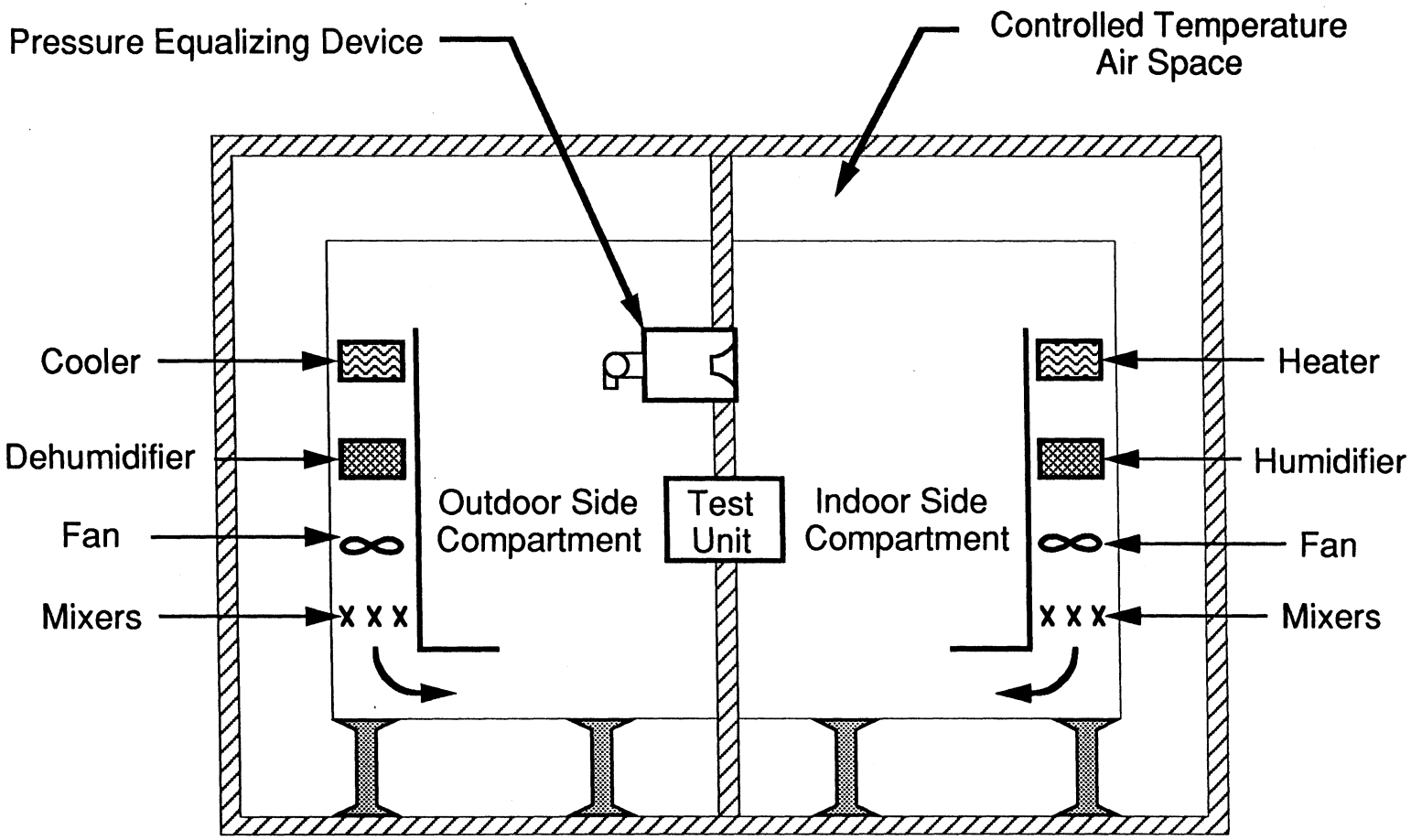

Figure 1.3 Balanced Ambient Room Calorimeter

2. DESIGN OF EXPERIMENTAL FACILITY

This chapter describes the design of an experimental facility for testing room air conditioners and split systems with capacities in the range of 0.5 to 2.5 tons of refrigeration (1.8 to 8.8 kW). As noted in Chapter 1, the point of departure for our design is ASHRAE Standard 16-1983 (ASHRAE 1984) which prescribes the requirements of a facility to be used for rating the capacity and energy efficiency of commercial units. However, the philosophy underlying the standard differs markedly from the goals of the present effort. Understanding this difference is essential for placing our design in proper perspective. Whereas the ASHRAE standard focuses on a single "rating condition" defined by specific dry-bulb and wet-bulb temperatures, our interest lies in being able to produce a wide range of operating conditions so that all important phenomena can be identified and understood. In addition, because our data are intended solely for use in research, they lack the legal implications which are of great concern in applying the standard. This difference permits certain simplifications to be made which reduce the cost and complexity of the facility without affecting our ability to obtain the desired operating data.

Besides the need to produce a wide range of operating conditions, we must also be able to directly measure several important internal operating parameters of the unit. These measurements include not only refrigerant loop conditions, but also local air temperatures, humidities and flow rates. Because our data are of an inherently diagnostic nature, the level of detail required is far greater than the standard considers. Indeed, the ASHRAE standard does not address internal measurements at all because no instrumentation of the unit is permitted during a ratings test.

Facilities specifically designed for carrying out the ASHRAE ratings tests are available commercially at costs ranging between $250,000 and $500,000. Not only are these sums beyond the means of our project, but such commercial facilities lack the versatility we need to develop a rich set of detailed data over a wide range of conditions. Our facility was ultimately constructed for roughly one tenth the cost of a similar commercial facility.

Despite the inherent differences between the philosophy underlying the ASHRAE standard and the goals of our project, the standard does provide valuable guidance in selecting equipment and in setting tolerances for instruments and controls. Moreover, the ability to conduct tests at the rating condition is quite important, since it allows us to compare our results with those obtained by the manufacturer of the unit. In addition to using the standard as a guide, we also visited manufacturers to study their facilities

and to take advantage of their many years of experience in conducting ratings tests. These visits proved very valuable in focusing our efforts and in providing insights into how one might best design and control a facility of the type desired. In some cases, these ideas were directly transferable to our design, and, in others, the idea was modified to accommodate our somewhat different purpose.

2.1 Design of Indoor Room

2.1.1 Physical Attributes

As noted in Chapter 1, we opted for the simpler and less costly calibrated-calorimeter method wherein the heat transfer from the indoor room is determined as a function of the ambient temperature. We improved on this basic concept by employing heavily insulating walls which limit conduction heat loss to no more than 100 W even for largest expected temperature differences. The uncertainty then in the ultimate energy balance rests on the *error* in determining the rate of energy loss through the walls. Inhomogeneities in the environmental conditions and uncertainties in the calibration procedure combine to give an uncertainty of no more than 10 W in the parasitic heat exchange even under the worst-case conditions. For the smallest units, this error in heat exchange through the walls translates to an error of less than 0.5 % in cooling capacity.

The walls of the indoor room are composed of four layers of polyisocyanurate foam insulation with a total thickness of approximately 12 in. Since this foam has an R-value of 7.2 (hr-ft^2-°F/Btu) per inch, the total R-value for the walls is approximately 86. These insulating foam walls are entirely supported by a aluminum unistrut frame located completely within the indoor room. This method of support eliminates virtually all wall penetrations along with their associated conduction and infiltration heat losses. In fact, the only penetrations through the wall are made by the electrical supply and instrumentation wires contained in PVC conduit. The conductivity of PVC conduit is smaller than that of traditional steel conduit, and, hence, conduction heat exchange is minimized to the maximum extent possible. Moreover, each of these conduit penetrations is carefully sealed around its circumference at the point where it exits the wall to prevent infiltration and moisture absorption into the foam. The penetrations are also stuffed with insulation and sealed with silicone caulk on both sides of the wall to prevent infiltration through the conduits. These measures provide an indoor calorimetry chamber with a very low heat transfer as is verified experimentally in Chapter 3.

Throughout the design and construction, we sought to exclude all moisture-absorbing materials from the indoor room and to carefully seal the walls to eliminate all paths for moisture transfer. The walls are built of four layers of foam board which are glued together. The outer three of these layers are faced on both sides with aluminum foil. The inner layer, which is in direct contact with the moist air of the indoor room, has a heavy embossed aluminum laminate facing. As each layer was applied, the joints between the foam boards were carefully sealed with silicone caulk and then covered with aluminum foil tape. The careful sealing of each layer of foam as well as the heavy aluminum laminate on the inner wall provides an effective barrier against moisture transfer.

The partition wall between the indoor and outdoor rooms contains two removable sections of similar design. One provides a doorway for accessing equipment in the indoor room. The other, illustrated in Fig. 2.1, is a window for mounting the test air conditioner. A foam collar, constructed by overlapping layers of foam board in a bank-vault fashion, is sealed directly to the housing of each air conditioner to be tested using silicone sealant. The unit and the foam collar together form a plug which fits tightly into the opening in the partition wall. The combination is rolled into place using a cart which is counterweighted to offset the torque created by weight of the cantilevered air conditioner. Gasket material is applied to the mating surfaces on the partition wall so that the collar can be firmly sealed in place. The gasket material is made of a closed-cell neoprene foam with a very low water absorptivity. Since only a small amount of gasket surface area is exposed to the indoor room, the effect of the gasket on heat and moisture exchange is minimal.

The plug is sealed into place using a clamping system which consists of a steel unistrut frame with bolts 6 in. long spaced at 1 ft. intervals around the perimeter of the opening as shown in Fig. 2.2. A rectangular annulus made of polycarbonate sheet stock distributes the force of the bolts uniformly around the edge of the opening. The uniform compression of the gasket material provides a very tight air lock. Moreover, the bank-vault style ensures that the opening is virtually leak-free.

2.1.2 Heat Addition and Air Distribution Systems

To determine the sensible cooling of a test air conditioner, heat is added to the indoor room such that the room is maintained at a steady-state temperature. At this steady temperature, we know that the amount of heat being added to the room is equal to the amount of heat being removed by the air conditioner plus the amount of

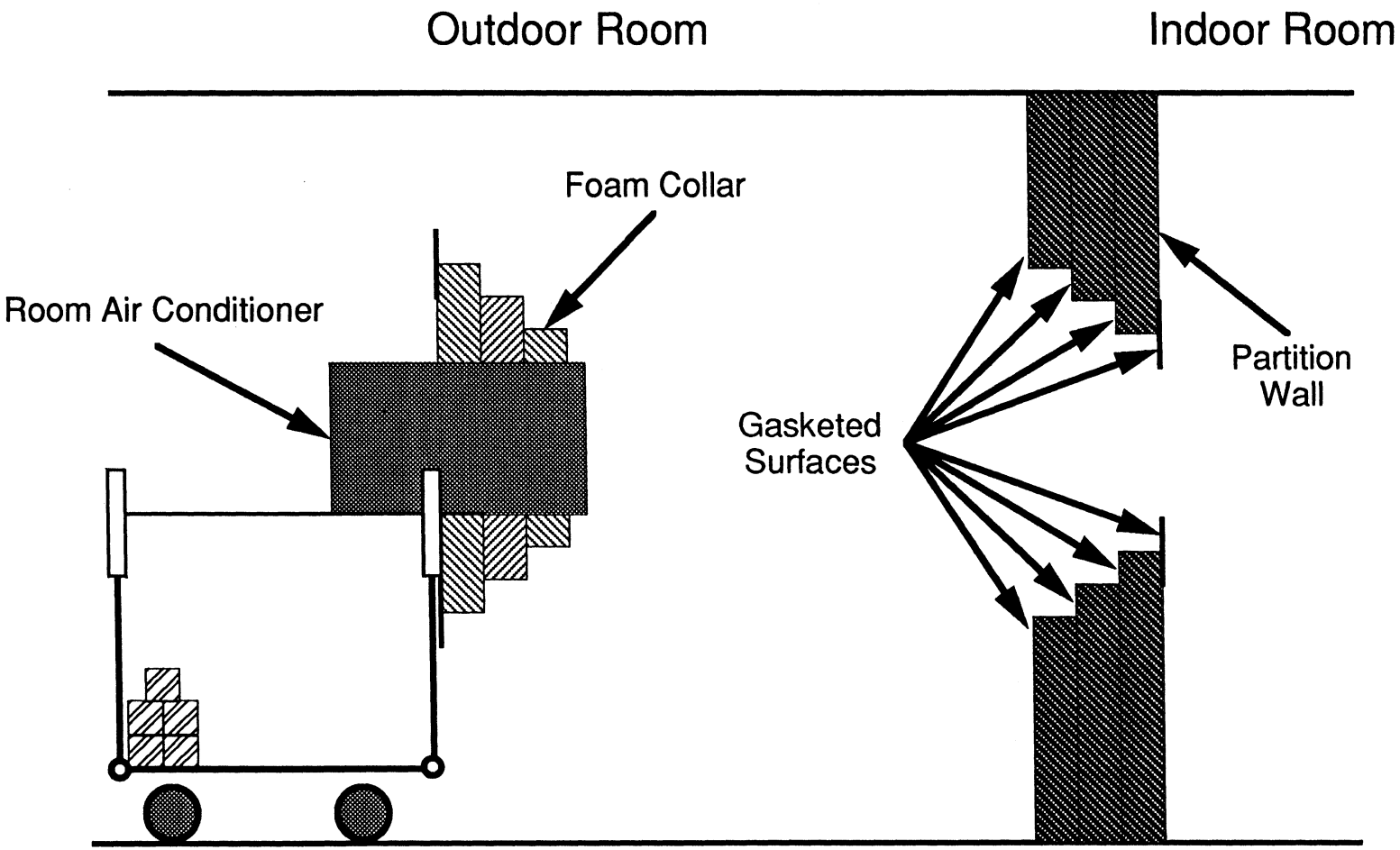

Figure 2.1 Gasketing of Room Air Conditioner Window

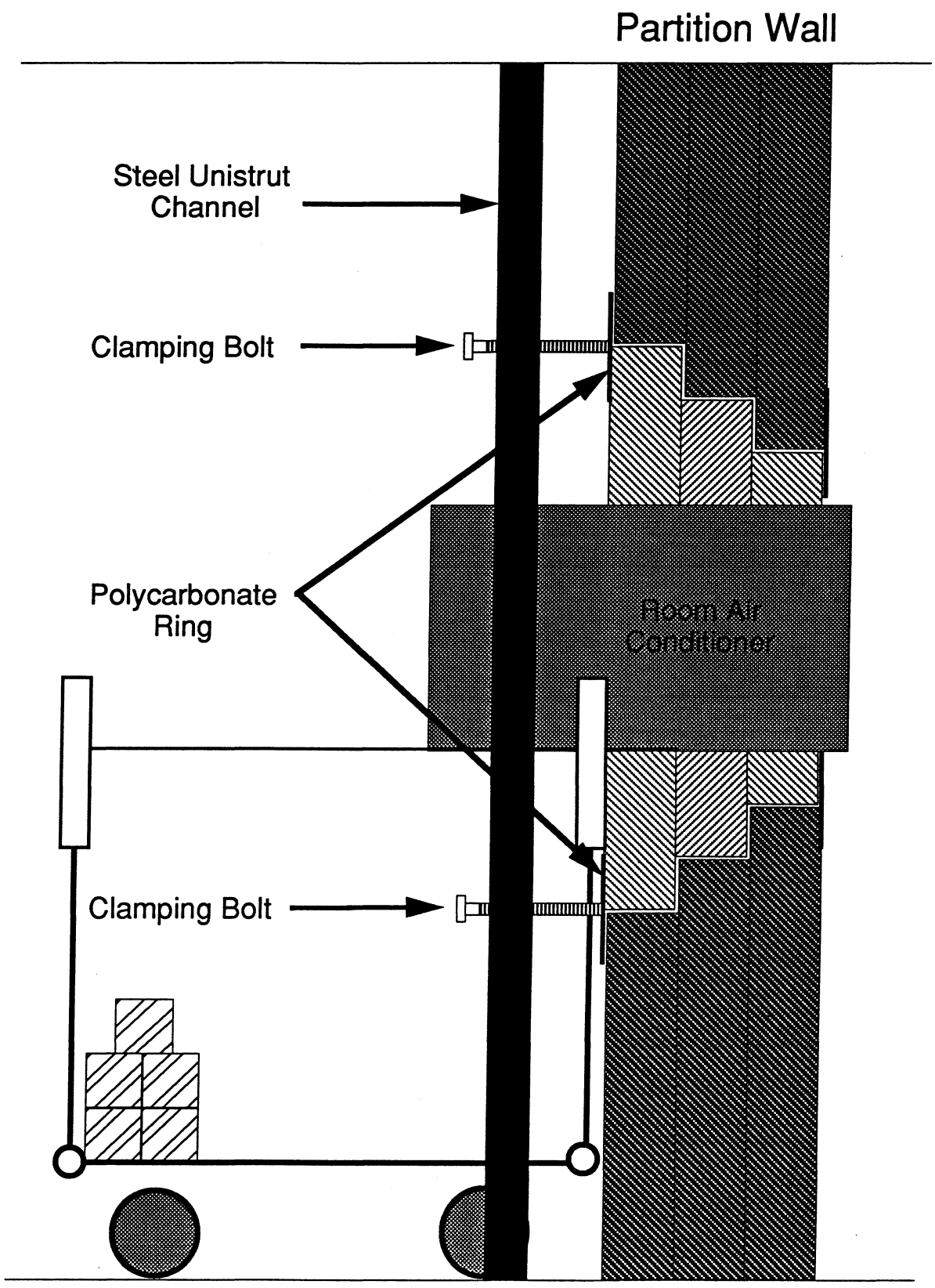

Figure 2.2 Clamping of Room Air Conditioner Window

heat which is lost through the chamber walls. We can calibrate the total heat loss from the room and measure the amount of power consumed by the electric heaters to determine the total sensible cooling achieved by the air conditioner.

2.1.2.1 Heat Addition System

The facility must be designed to test air conditioners rated from 0.5 to 2.5 tons (1.76 to 8.8 kW) of cooling, which dictates supplying a continuously variable heat load over this range to balance a 100% sensible cooling load. The maximum heat loss through the walls will be on the order of 100 W, which must also be supplied by the heating element. We sized our maximum heat input requirement to be 10 kW based on the capacity of the test units, the maximum heat loss from the room, and the consideration that the units might have larger capacities at non-rating conditions. Continuously varying the heat load can be achieved easily by using a time-proportional control system, which will be discussed later.

The first method that we investigated for adding heat to the room was to use 1 ft by 4 ft silicone mat heaters mounted on aluminum plates a few inches away from the walls of the chamber. These would be uniformly distributed along the walls and would therefore add heat to the room in a uniform manner. Fans would be added to the system to assist the heat transfer to the air and to meet the ASHRAE standard for air circulation in the room. This idea, however, was not incorporated because we realized the potential benefit of using an electric furnace for heat addition. The furnace provides a packaged unit containing a blower and a resistance coil mounted in a steel duct. This unit is significantly cheaper than a system of plate heaters and was much more convenient to implement into our facility.

The electric furnace is to be controlled to yield a steady-state temperature in the indoor room. The control system schematic is shown in Figure 2.3. Voltage signals from the two RTD's in the indoor room are averaged by an analog circuit before being read by the microprocessor controller. The circuit receives the two voltage signals and, using instrumentation amplifiers, translates them into single-ended voltages with respect to the same ground. These signals are then routed into a standard summing operational amplifier circuit, which combines the signals. Subsequently, the summed voltage is divided by means of a potentiometer to yield a scaled value that is read by the controller. The controller compares this average temperature to the setpoint temperature and follows a PID algorithm to send an output signal to a solid state relay. This relay is placed in the heating element power supply line so that power can be

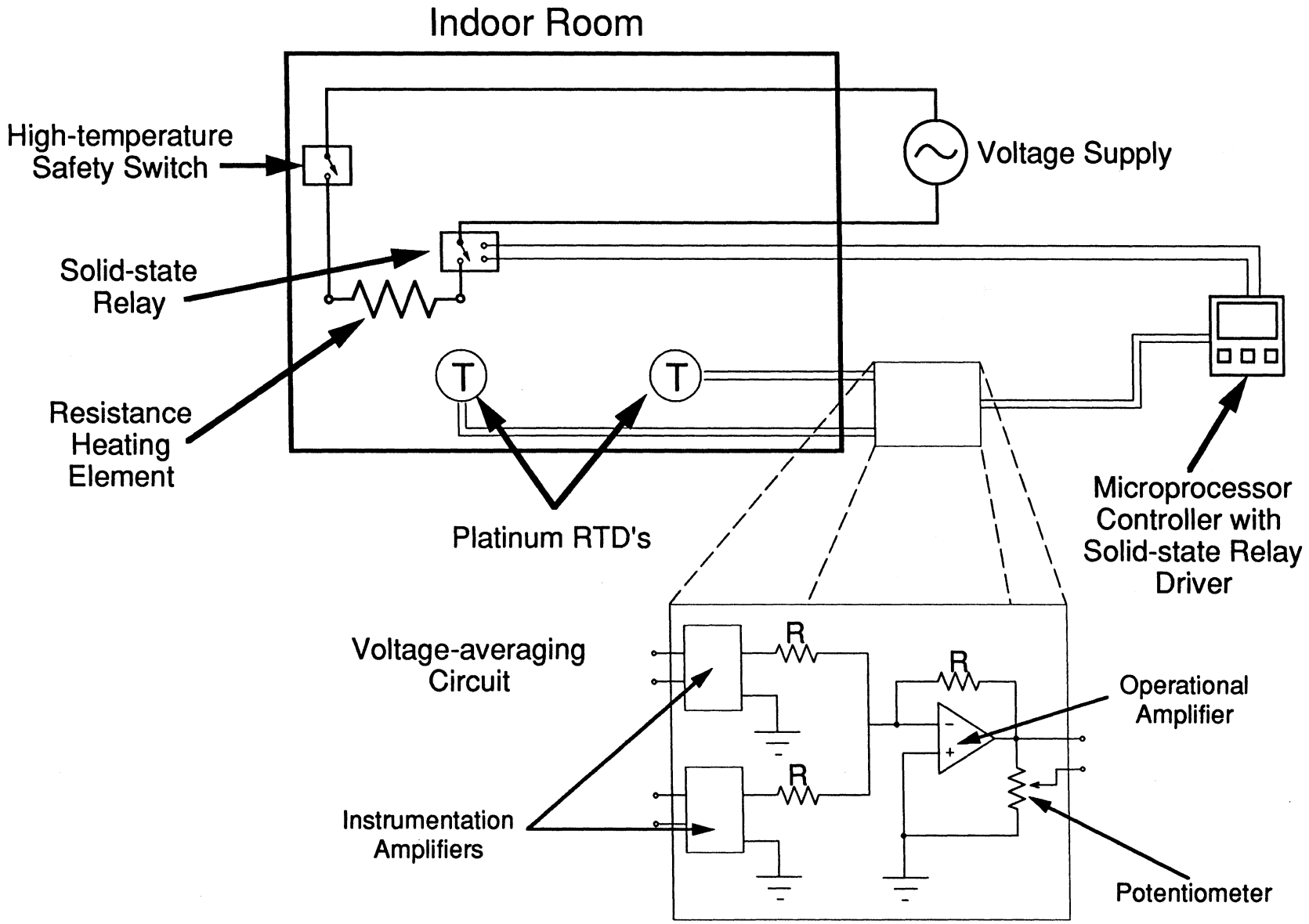

Figure 2.3 Furnace Control System

time-proportionally applied to the element. The controller will drive the relay closed for a certain percentage of its duty cycle, and then open for the remaining percentage to modulate the amount of heating done by the resistive element. The percentage of the duty cycle for which the relay is closed is determined by the controller PID algorithm based on the setpoint and room temperatures. Using this control system, one can maintain a constant average temperature in the indoor room. Figure 2.3 also shows a high-temperature safety switch in the heating element power line which terminates power to the element if the furnace high-temperature limit is exceeded.

Measurement of the power consumed by the electric furnace (and the humidifier, which is discussed in later sections) will be accomplished by a device which is designed for power measurement of non-standard waveforms, including "chopped" waveforms. This system will be detailed in a forthcoming document by Feller (1993). The accuracy of the power measurement device is expected to be 0.5% of the maximum input power.

2.1.2.2 Air Distribution System

A system for controlling bulk air movement, velocity and uniformity has been designed and built within the indoor room. As specified by ASHRAE Standard 16-1983 (ASHRAE 1984), circulation within the test room must be at least twice the circulation of the evaporator fan, and great enough to create at least one room air change per minute. Of the room air conditioners we will be testing, the greatest evaporator fan circulation will be 700 cfm. Since our room has a volume of only 700 ft^3, the number of room air changes per minute is not a limiting factor. We sized the fan in our furnace to circulate air at 2000 cfm, which provides a decent cushion over the ASHRAE specification. The actual air flow rate is slightly less than the rated flow because our distribution manifold introduces a minimal pressure increase at the furnace outlet. This effect is described later in this section.

The ASHRAE standard also specifies that the air velocity in the chamber within three feet of the face of the air conditioner be less than 100 fpm. In the indoor room, we have built an integrated intake and outlet plenum for the furnace. This system, which is situated opposite the room air conditioner against the rear wall of the chamber, is shown in Figure 2.4. The furnace is shown in the center of the diagram with its heating element and blower. This system takes advantage of buoyancy-driven circulation to control bulk air movement, by forcing the warm air out at the bottom of the room and drawing the cooler, mixed air in at the top. The blower draws air from

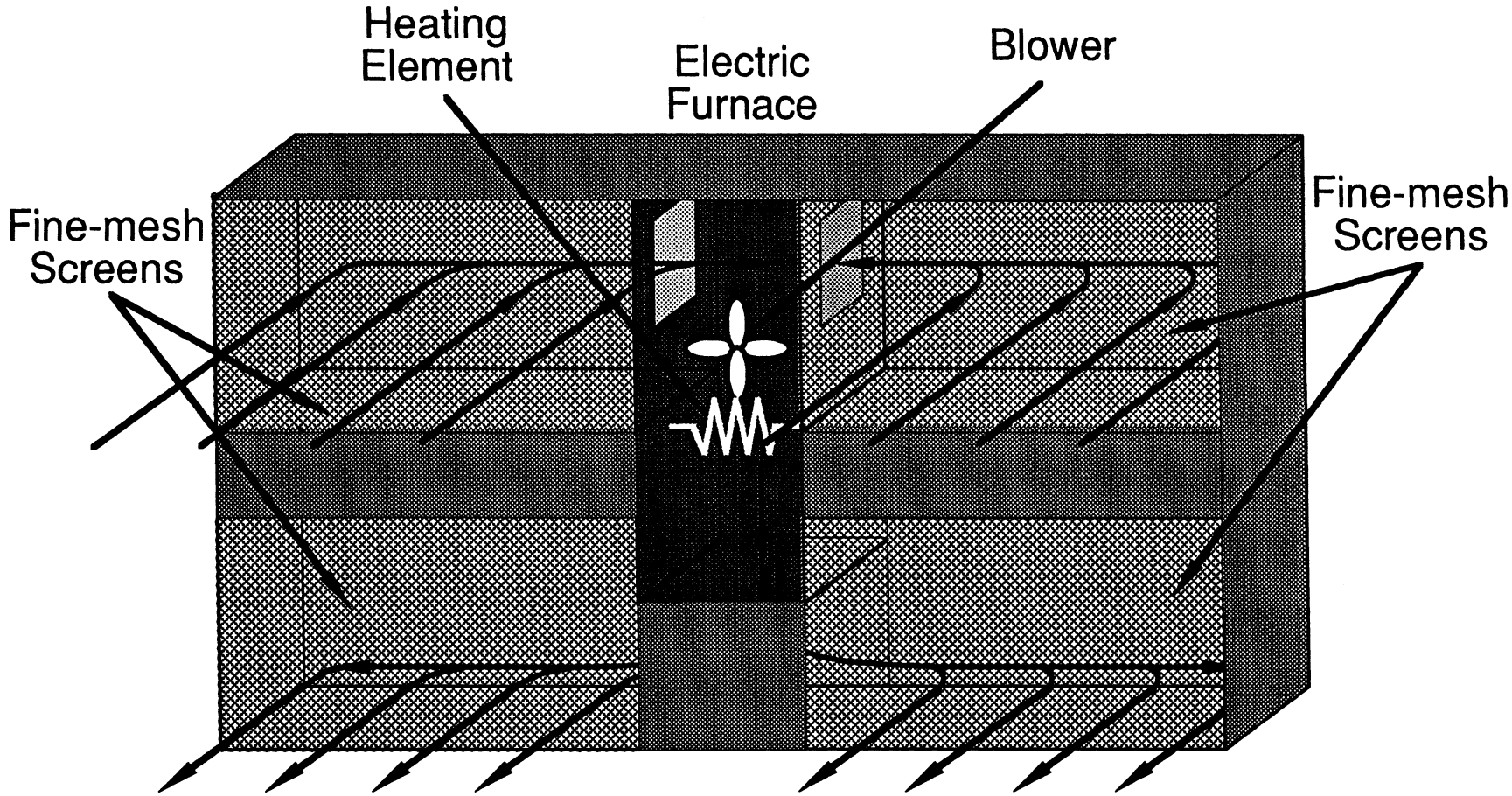

Figure 2.4 Indoor Air Distribution System

both sides of the room through vertical fine-mesh screens, into a plenum, and then down through the furnace. Air exits the furnace from below and is routed to the sides into separate plenum chambers. From there the air emerges through another set of vertical screens back into the room. By using the exit plenum chambers as diffusers, the exit air velocity is reduced to a value well below the specified 100 fpm limit within three feet of the air conditioner face.

By using screens on the face of each exit plenum, a great resistance to flow is presented to the furnace exit air in the direction perpendicular to the screen. This causes the air to move longitudinally in the plenum duct. As long as the frictional pressure drop induced by the walls of the plenum is much smaller than the pressure drop introduced by the screen, the flow will have a tendency to move along the plenum and fill the chamber before being forced to exit through the screens. Since the chamber will fill before the air exits, the face velocity at the screens will be very uniform. A similar argument can be used to explain the use of plenum screens at the inlet to the furnace, and their contribution to velocity uniformity within the room. The screening material was chosen based on its airflow resistance characteristics. The flow resistance coefficient R_f is defined as

$$R_f = \frac{\Delta P}{\frac{1}{2}\rho_g V_m^2} \tag{2.1}$$

where ΔP is the pressure drop across the medium and V_m is the mean velocity through the medium. For screening material, a correlation exists relating the resistance coefficient to the flow and geometric parameters. This relationship is defined as

$$R_f = 6\left[\frac{(1-\delta)}{\delta^2}\right] Re_w^{-\frac{1}{3}} \tag{2.2}$$

where the Reynolds number based on screen wire diameter Re_w is defined as

$$Re_w = \frac{\rho_g V_m d_w}{\delta \mu}. \tag{2.3}$$

δ is defined as the ratio of screen open area to total area and d_w is the screen wire diameter (Gavin, 1983). We calculated resistance coefficients for several different

commercially available screens in order to compare them with the resistance coefficient of air moving along the plenum as if it were a simple duct. The resistance coefficient for a duct is defined by

$$R_f = \frac{f\,L}{D_h} \tag{2.4}$$

where f is the Moody friction factor, L is the length and D_h is the hydraulic diameter of the duct. We selected a screen such that its resistance was three orders of magnitude larger than the frictional resistance along the duct. This assures adequate filling of the plenum before the air is forced into the room. We also checked the pressure drop imposed by the screens to be sure that we would still meet our required flowrate. The total back pressure imposed on the system by all four screens was calculated to be less than a tenth of an inch of water. Although this pressure does slightly reduce the airflow capacity of the furnace, the ASHRAE standard requirements for airflow are still easily met.

2.1.3 Moisture Addition Systems

One method for determining the moisture removal capability of a test air conditioner involves maintaining a constant humidity in the indoor room by adding water vapor at the same rate as it is removed by the air conditioner. By holding humidity constant and by either (a) calibrating moisture leakage from the room or (b) assuming it to be negligible, one can determine the moisture removal rate of a unit by measuring the rate of moisture addition to the indoor room.

Using a system simulation model, we estimated the maximum test unit moisture removal rate to be 27 lb_m/hr. This calculation was made assuming the largest capacity unit and a saturated (100% RH) indoor room condition. Thus, the humidifier must be able to supply water vapor at a continuously variable rate between 0 and 27 lb_m/hr to meet the removal requirements of any test unit at any given psychrometric state. Aside from this condition, the only other design constraints imposed on the system are qualitative in nature. For instance, the humidification system should be packaged so as not to significantly disturb the air circulation in the room, or otherwise affect indoor room performance. The moisture should be distributed low within the room and pass in front of the exit of the reconditioning equipment. In this manner, water vapor is released into the warmest air in the chamber, which has the greatest

ability to hold moisture. Also, if it is released low in the room, the vapor will travel further and mix more thoroughly with the hot air stream exiting the plenum before reaching the ceiling of the chamber. This reduces the chance of water vapor condensing on the chamber surfaces.

The humidifier must be well integrated with a system for determining the rate at which it adds moisture to the indoor room. For this reason, all the considered humidification options involve concurrent consideration of measuring systems. Ideally, we desire the accuracy of this system to be perfect since the smallest required moisture addition rate is 0 lb_m/hr, and any small deviation from the actual rate will create a theoretically infinite percentage error. However, a small error, such as 0.1 lb_m/hr for a measurement of 27 lb_m/hr, yields a tolerable error of 0.37%. It is difficult to assign a percent error limitation to the system, since its capacity changes depending upon indoor psychrometric conditions and the dehumidifying ability of the test unit. Instead of designing the system for a tolerable percent error, as is done in a single capacity system, we searched for the most accurate measuring device which, when coupled with a reasonable humidifier design, yields a low-cost solution.

2.1.3.1 Heated-Plate Systems

One of the first ideas we investigated was to drip water onto a heated plate at a desired flowrate. The temperature of the plate is set at a certain value above the boiling temperature. As water is dripped on the plate, it evaporates quickly. As the moisture demand increases, more water flows onto the plate and consequently heat transfer from the plate to the water increases as the temperature controller attempts to maintain a constant plate temperature. Assuming there is enough heater surface area to effect the heat transfer required for evaporation, the main advantage of this system is its quick response time. As long as water does not accumulate on the plates, response time is low since energy is not consumed in heating the resident water, but only in evaporating immediately incident water.

Figure 2.5 shows another variation of this idea which involves encasing the heated plates in an insulated chamber. This approach allows the air in the chamber to remain at a temperature higher than the boiling point of the water. When the water evaporates off the plate, heat transfer from the air to the water vapor serves to superheat the vapor. This method reduces the chance of moisture condensing after it mixes with the air in the indoor room.

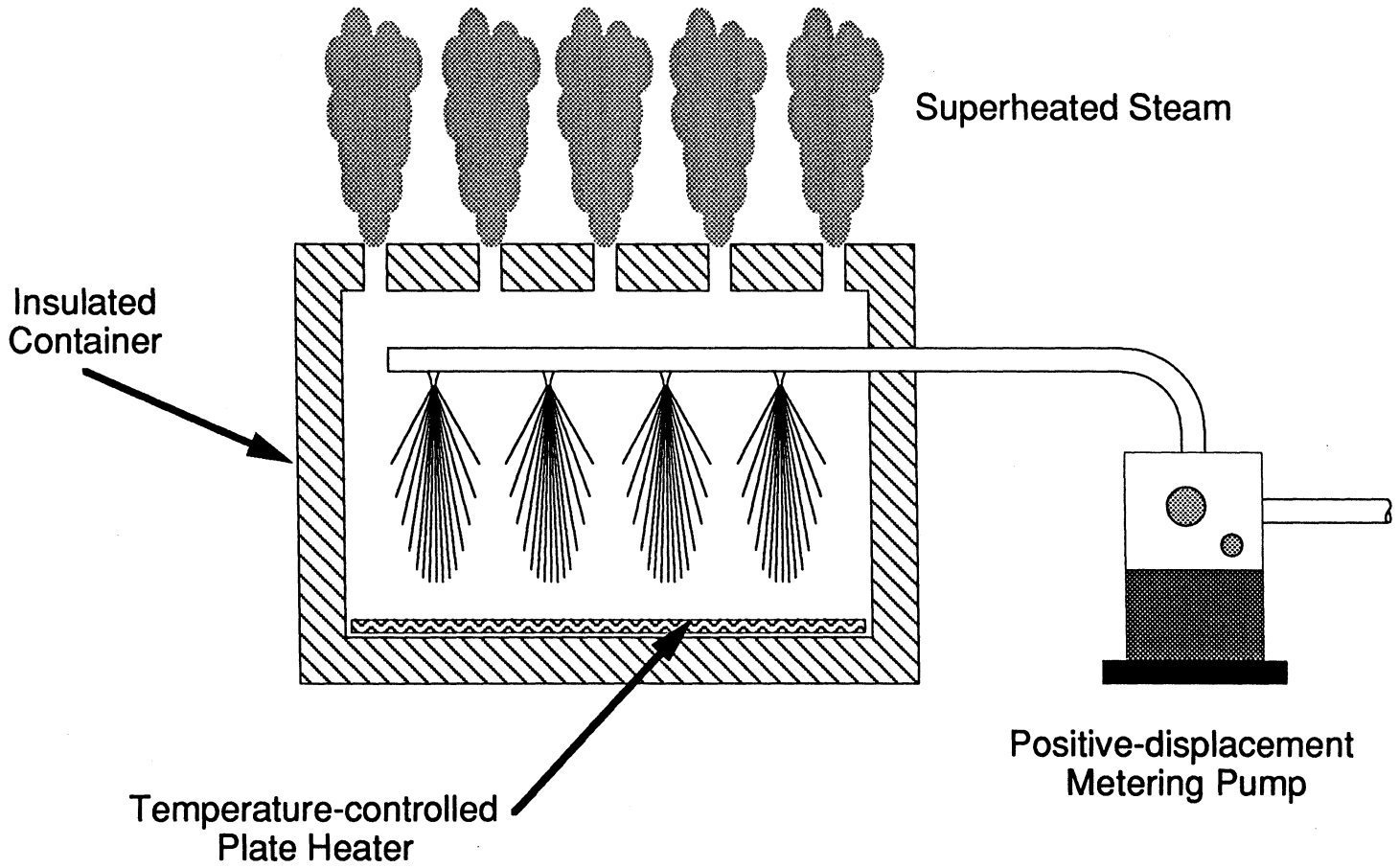

Figure 2.5 Hot Plate Humidifier

We investigated two methods for metering water onto the plate. The first of these, shown in Figure 2.5, uses a positive-displacement pump. Positive-displacement pumps force a fixed volume of fluid through the pump for each rotation of the shaft, thus making them accurate flowrate metering devices. The pump that we considered for this purpose was a diaphragm pump with a manually controlled stroke length and a remotely controlled stroke rate (using a 4-20 mA signal). Using this system, we can calibrate the flowrate at each manually set stroke length for a range of stroke rates, and expect an accuracy of ±2% of full scale. By setting the stroke length to a value which would allow a varying stroke rate to cover the full range of flowrates needed for testing a particular air conditioner, full control is achieved remotely. A process controller reads the indoor room humidity, compares it to the setpoint, and sends a 4-20 mA signal to the pump to modulate the water flowrate. The problem with this system is that positive displacement pumps cannot provide flow at rates approaching 0 lb_m/hr. In general, we found that these pumps will not provide consistent flow in the range of 0-5% of full scale output. This poses a problem for us in testing air conditioners at conditions which result in low moisture removal capacity.

The second option for metering water onto the heated plate involves the use of pressurized water or a pressurized air/water mixture. One of these types utilizes an air pressure driven, variable capacity liquid injection system. This system injects bursts of water based on the pressure setting. The duration of these bursts can be varied to yield the desired flowrate. Again, we would need to control two variables in order to set the flowrate. First, we must control the air supply pressure and, second, we need to control the timing of the water bursts. To maintain constant humidity, we also need to control a third variable, the plate temperature. Since it is necessary to control three separate variables, we decided not to pursue this approach.

A similar idea utilizes a spray nozzle instead of the injection system. We investigated water-pressure driven and air-pressure driven atomizing spray nozzles to determine their suitability for humidity control. The advantage of these nozzles is that they produce very small droplet sizes which are easily evaporated either on a hot plate or in warm air.

As part of the heated plate idea, we proposed using the spray nozzles as the distribution mechanism in place of the fluid injection system. For this system we chose a hydraulic atomizing nozzle, because its flowrate can be controlled solely by the water pressure. Although the air atomizing nozzles produce small droplet sizes, their smaller size does not hasten evaporation from the heated plate enough to warrant involving another control variable; namely, air pressure. Spraying water onto the

heated plates for evaporation is fairly easy to calibrate since the flowrate can be varied by regulating the water pressure. However, at lower pressures (and consequently, lower flowrates) the nozzles no longer produce the small (0.040 in. diameter) droplets which evaporate quickly. This system can be modified to pulse water intermittently through the nozzle at higher pressure. This approach solves the droplet size problem but also introduces another control variable; namely, pulse duration. An even greater problem lies in trying to measure the amount of water that is being used by the system when the flowrate is discontinuous. One approach we considered was to time the bursts and then use a calibration of water flowrate vs. pressure to calculate the actual flowrate. The need to use such a calibration makes this approach a difficult and potentially inaccurate measuring system.

2.1.3.2 Misting Systems

As alluded to previously, we also entertained a completely different humidification idea based on spray nozzles. Instead of adding heat directly to the water, we considered spraying a fine mist into the air in the indoor room and allowing heat transfer from the air to evaporate it. In effect, we are using a form of evaporative cooling. Our heating system in the indoor room is sized to balance the total capacity of the largest test unit. Whether the cooling is purely sensible, purely latent or a mixture of the two, the cooling capability never exceeds the capacity of the unit. Since the heater is controlled to maintain a particular temperature in the room, it must add enough heat to balance both the sensible cooling load of the air conditioner and the evaporative cooling load of the humidification system. The heater must also be sized large enough so that it can provide enough heat for the sensible and latent loading of the air conditioner. This approach eliminates the need to buy, use and control ancillary heaters.

The air atomizing nozzles yield much finer droplet sizes than their hydraulic atomizing counterparts, and the particle size can be reduced by increasing the air pressure. Using these nozzles, we could keep the water pressure constant and vary the air pressure to control the flowrate and droplet size. The water flowrate decreases as the air pressure increases. Assuming that, at our maximum flowrate, the droplet size is sufficiently small for evaporative cooling, an air-pressure regulator can be used in concert with a controller to meter the necessary water to the nozzle. If the process runs at a continuously variable rate, it can be calibrated fairly simply by accurately measuring flowrate vs. air pressure at the operating water pressure. The drawback to

using this system for controlling the flowrate is that as pressure is increased, the length of the nozzle spray pattern increases. In fact, it becomes so large for the size system we need that we cannot fit the nozzle with its associated spray pattern inside our chamber. The droplet plume will reach and wet the wall of the chamber. We certainly cannot have water building up as liquid in the chamber, since our moisture balance assumes that all water entering the humidification system adds to the moisture content of the air.

2.1.3.3 Reservoir Systems

Commercial Humidifiers

One of the more obvious solutions to this humidification problem is to buy a commercially available humidifier. We investigated some steam generating humidifiers and were able to find a system whose manufacturer claimed that their device can cover our full range of flowrates. As an option with this humidifier, we could purchase an SCR control system which claimed to be able to control relative humidity to within 2%. The cost of the system including controls was roughly $5000. But, after having invested $5000 into this system, we still would not have achieved any ability to measure the moisture flow rate. The second control option offered was a time-proportioning system which can control humidity within 5% at two-thirds of the cost. However, the accuracy of this system is much too low for our purpose. Since the humidifier is inseparable from its control system, and we can easily build the actual humidification device ourselves (a ten gallon tank with two to three immersion heaters), we decided not to pursue this idea any further.

A second commercially available solution that we investigated was the purchase of an electric boiler. With this approach, we would place the boiler outside the indoor room and funnel the steam into the room through a pipe in the wall. Throttling the steam would be accomplished by either (a) venting part of the steam to the ambient, (b) controlling the power input to the heating element or (c) a combination of these two. We can measure the steam using a vortex-shedding flowmeter which is very accurate at higher steam flowrates. However, because it is very difficult to sense the vortices at low flowrates, this method becomes ineffective over our full range of flow and was not used in our facility.

Steam Pots

One idea we experimented with was inspired by the test facilities of one of our research sponsors. Their setup consists of a bank of steam pots as shown in Figure 2.6. Each of these steam pots consists of a piece of two-inch copper tubing with one end bushed down to accommodate a screw-plug immersion heater. The steam pots are then insulated and linked together in parallel by a horizontal piping network, which is connected to a supply tank. Water level is controlled using an identical but unheated vessel in parallel with the steam pots. Since the level-control vessel has no heater, the water surface is not agitated and this fact allows for accurate level control. The level-control system is also shown in Figure 2.6. Two wires lead into the level-control vessel, one of which is submerged in the water all the time and another which marks the reference height. A DC voltage supply is connected through a 10MΩ pull-up resistor across the wires and a hex converter chip. When the water level drops below the shorter wire, current no longer flows through the water to complete that side of the circuit. At that point, the line current is drawn to ground through the high impedance offered by the hex converter and the 10 MΩ resistor. This results in a negligible current flowing through the circuit, which yields a small voltage drop across the resistor and hence a CMOS logical high input to the hex converter. The hex converter translates the CMOS logical high to a TTL logical high of 5 V, which energizes a solid-state relay. The relay closes the power supply circuit for the solenoid valve and thus energizes the solenoid and opens the valve to allow the steam pots to fill. When the level reaches the reference height, a comparatively large current flows through the water to ground, because the resistance of the water is many orders of magnitude smaller than the input impedance of the hex converter. This relatively large current causes a correspondingly large voltage drop across the 10MΩ resistor and brings the hex converter input voltage down to a CMOS logical low. Consequently, a zero voltage signal is sent to the relay, which opens the solenoid circuit and thus closes the flow control valve. This system results in very frequent switching of the solenoid and, consequently, very tight control on level.

The evaporation rate is controlled by time-proportioning full power to the immersion heaters. A microprocessor controller, responding to a difference between a relative humidity setpoint and the sensed value, drives a solid-state relay that is connected in parallel with the immersion heaters. By switching the solid-state relay on for a certain percentage of its duty cycle and off for the remaining portion, the heat output is controlled to be that same percentage of the heat load at full power. This

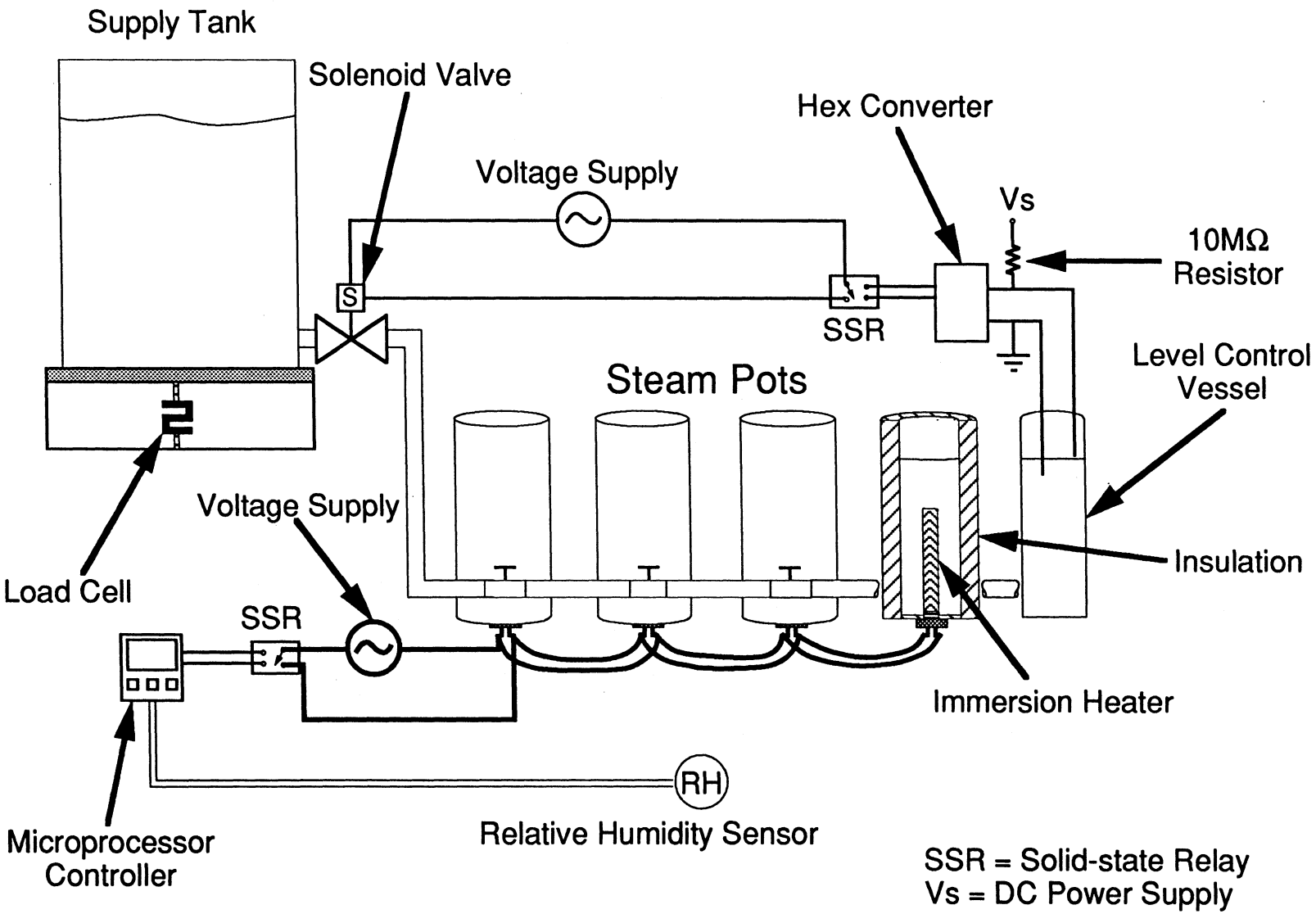

Figure 2.6 Steam Pot Humidifier

allows for the continuously variable evaporation rate needed for testing the full range of systems over the full range of psychrometric conditions.

The amount of water evaporated can be obtained by measuring the change in weight of the supply tank with a load cell as shown in Figure 2.6. At a steady-state condition in the room, the evaporation rate will be constant and by taking weight data over time, we will be able to get an accurate representation of the evaporation rate produced by the steam pots.

We experimented with designs for the steam pots to determine their viability in our situation. We built a steam pot out of copper tube, screwed in an immersion heater and applied power to the heater. We found that the water in the tube boiled uncontrollably unless the heat input from the immersion heater was less than 500 W. Our first reaction to this discovery was to conclude that the uncontrollable boil was due to the high watt density of the heater. We hypothesized that too much heat was being transferred to a surface area of water that was too small. This was causing large gas bubbles to form on the heater. We obtained and tested another heater which had a watt density that was one-half that of the first. The results of this test were the same as for the first heater and the steam pot still spit liquid water from its top. We tried lengthening the steam pot and adding more water to it ,but this change in water volume had only a small effect on the boiling characteristics. The watt density did not seem to be the problem, or at least not a problem we could solve within the constraints of standard copper tubing and available immersion heaters. More likely, the problem was that we were adding too much heat to too little water.

Our application calls for 27 lb_m/hr of steam production for the worst case test scenario. This means that a total of 7.7 kW (26.2 kBtu/hr) of heat must be added to saturated liquid water to meet this evaporation rate. If we are limited to 500W input to any one steam pot, this dictates a need for 16 of these steam pots. This would mean a big, bulky apparatus within our test chamber, not to mention the expense involved in buying the 16 heaters and the parts necessary for building the bodies of the steam pots. For these reasons, we decided to try another idea.

Barrel Humidifiers

Our next and final idea was aimed at solving the problem of uncontrollable boiling and finding a simplistic, foolproof and inexpensive method of adding moisture to the indoor room. The obvious way to eliminate the uncontrollable boil is to increase the amount of water in the boiler. We decided to build a system utilizing a 24 gal steel

drum as a boiler. The basic design for the boiler is shown in Figure 2.7. We welded four couplings to the cylindrical side of the drum six inches from the bottom and installed a 2 kW immersion heater in each of them. After attaching two inches of polyurethane insulation to the outside of the drum, we coated the inside with rust-preventing primer and high-temperature paint. On the drum lid we mounted an insulated piping network, which leads through a U-bend to the steam outlet. We wrapped temperature-controlled tape heaters around the U-bends so that we can evaporate the condensation from the tube walls, all of which will drip into the U-bend. This will assure that any water leaving the drum will also leave the pipes. The significance of this fact will become evident in the discussion of the moisture addition measurement system.

Before actually building the system described above, we tested the steel drum as a boiler and encountered rusting problems. At first, we coated the inside of the drum with a rust-preventing primer and a high temperature paint as mentioned previously. After boiling for the first time in the drum, it began to rust severely. We sanded off the rust and any loose paint and applied a cold galvanizing treatment over the paint (as recommended by the manufacturer). After boiling for a day and allowing the boiler to cool, we noticed that the paint behind the zinc galvanizing compound was peeling off in large flakes. We hypothesized that this might be due to the flexing of the drum caused by thermal cycling. To alleviate these problems, we searched for a coating which would be able to withstand boiling temperatures, moisture and thermal expansion of the surface. What we found was a coating which is made specifically for the inside of boilers. We stripped all the paint and primer off the drum, treated the bare metal with a phosphoric acid solution, and applied the coating several times as specified by the manufacturer. We had no peeling paint problems after initial testing, but the surface was retaining small amounts of iron-oxide. The rust did not seem to be penetrating the paint because it appeared only as a thin layer that was easily washed off with an abrasive sponge. After subsequent testing, we found the rust to be building up on the coating and becoming more prevalent all over the drum. The paint advertised an activation temperature of 200 °F at which it would become protective. This certainly takes no effort to reach during boiling. It may have been possible that during the start-up and cool-down phases, when the temperature was below the activation temperature, no rust protection was offered to the steel and this allowed the corrosion to occur. However, we were advised by the manufacturer that as long as the boiler was taken from ambient temperature directly to boiling point temperature, the coating would be activated and protection would be adequate during cool-down.

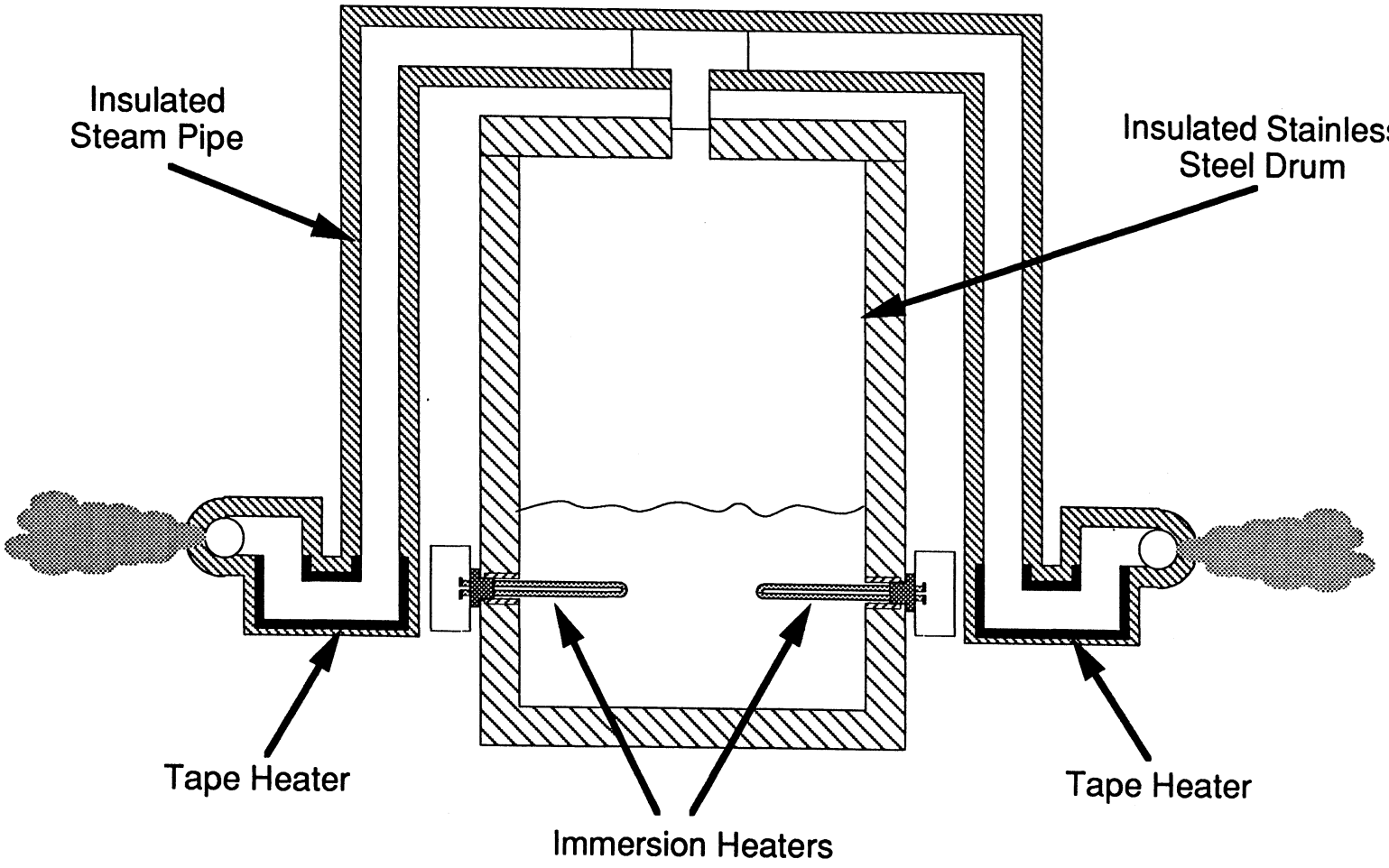

Figure 2.7 Drum Humidifier

Apparently, this was not the case and we decided not to put any more effort into rust-prevention coatings. To avoid the problem, we decided to buy a stainless steel drum as shown in the final design in Figure 2.7.

The humidification system is controlled to provide a steady-state relative humidity in the indoor room. This control system is similar to the furnace control system, as can be seen in Figure 2.8. Voltage signals from the relative humidity sensors in the indoor room are averaged by a circuit similar to that used by the heater control system. This averaged signal is compared to a setpoint, which causes the controller to drive a solid-state relay to modulate power to the immersion heaters in the humidifier. The humidity controller operates in the same way as the furnace controller. There is a low water-level safety switch built into the humidifier, which opens when the water level drops below the reference height. When this occurs, a float switch opens the energized circuit and the solid-state relay, which is in line with the switch, becomes de-energized. Since the relay will not be energized, it will cut power to the immersion heaters and keep them from overheating.

It should be noted that at the time of writing of this paper, we are not presently using the controllers to automatically maintain constant temperature and relative humidity in the room. An important feature of these controllers is the ability to manually set a power input to the electric furnace or immersion heaters. We have been using this feature to learn about the response of the indoor room to constant heat and moisture inputs. This approach will help us quantify the time constants associated with the heating and humidifying systems in the indoor room, and will allow us to develop "smarter" control algorithms.

2.1.3.4 Measurement of Moisture Addition

The method we are using to measure the steam flowrate is to weigh the boiler on a load cell and record the weight change over time. This method of measuring flowrate will be a fundamental measurement and is not subject to the inaccuracies involved in calibrating the measured value to an intermediate variable. The accuracy of this measurement, like many measurements, will depend on the maximum weight of the system. The lighter the system, the more accurate the measurement will be, assuming a fixed resolution of the reading device. The weight of a boiler will be a substantial fixed weight which must be measured using this weighing device. If the weight of the boiler was removed, a very accurate measurement of the water flow rate could be produced. As shown in Figure 2.9, by using a counterweight system to

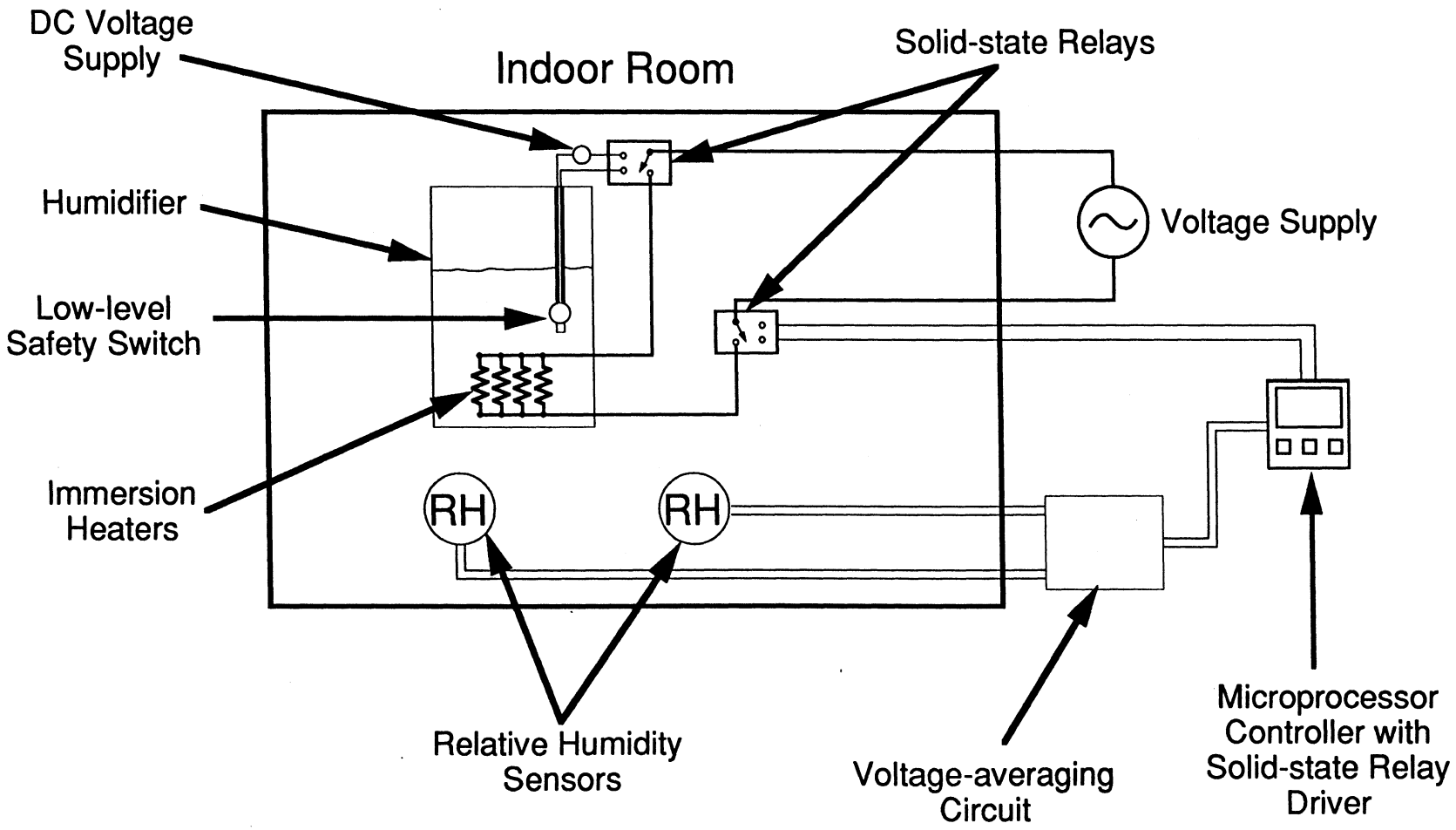

Figure 2.8 Humidifier Control System

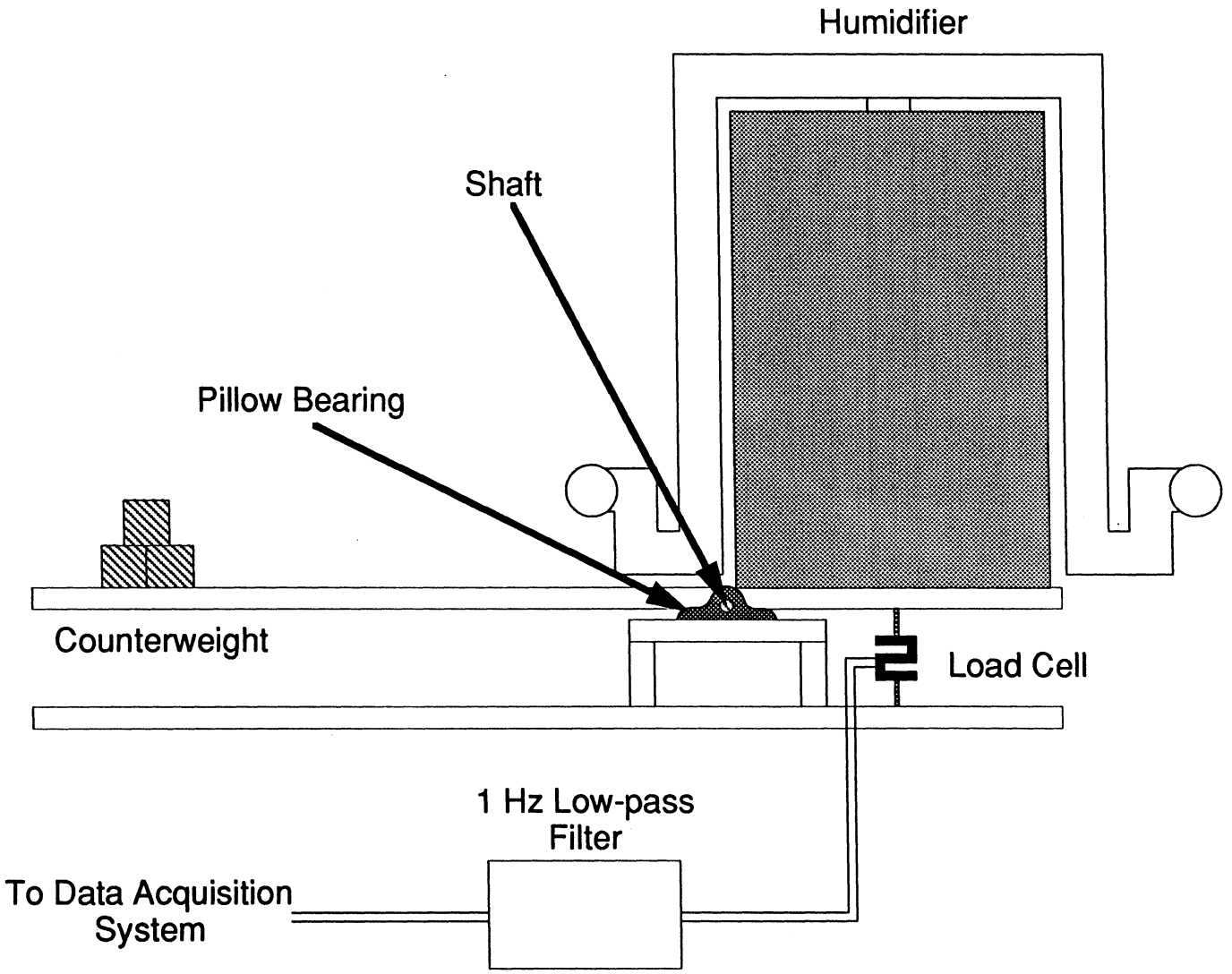

Figure 2.9 Moisture Addition Measurement System

balance the weight of the humidifier, we will be able to measure only the weight change of the water. This will increase the accuracy of our measurement by decreasing the required capacity of the load cell.

The counterweight system consists of a six-foot unistrut platform with a steel shaft mounted two feet from one end of the platform. This shaft is supported by a pair of pillow blocks with well-lubricated ball bearing inserts to allow for free movement of the platform. These pillow blocks are mounted to a firmly-planted unistrut base. A 50-lb_m capacity S-beam load cell is mounted in the span between the base and the platform directly underneath the humidifier. Counterweights are added to the balancing side of the platform so that the load cell only measures a maximum load of 50 lb_m.

We decided to buy a 50-lb_m load cell because 50 lb_m of water is more than sufficient to achieve a single steady-state psychrometric condition in the indoor room. This point is noted in light of the fact that the maximum evaporation rate which we predict necessary for steady-state operation is 27 lb_m/hr. In order to obtain other conditions during the same data run, it may become necessary, in some cases, to remotely fill the boiler from outside the chamber. This provision may be added to the system at a later date. By choosing the 50-lb_m load cell, we obtain an instrument with a 0.1% full scale accuracy or a total accuracy of 0.05 lb_m. The electrical response of the system is 3.1 mV per excitation volt at full scale. When we excite the load cell with a 15 V signal, this corresponds to a 46.5 mV signal at 50 lb_m. By using our Fluke 2280 datalogger, we can read this signal to 0.6 μV, which corresponds to reading accuracy of 0.000645 lb_m. Clearly, the limiting factor in total accuracy is the load cell accuracy. As shown in Figure 2.9, we condition the output signal with a 1 Hz low-pass filter, which is necessary to remove noise generated by oscillations in the system due to vigorous boiling.

2.1.3.5 Humidifier System Calibration

The position and orientation of the humidifier above the load cell is crucial to measurement accuracy. The moment arm measured from the shaft to the center of mass of the water in the humidifier must remain constant throughout the measuring range of the load cell. If this condition is not met, the weight measured by the load cell, as water evaporates from the humidifier, will be dependent upon the moment arm to the center of mass of the water, as well as the weight of the water in the drum. In order for the calibration curve to be linear, the humidifier must be level in the direction

along the see-saw platform and must not change position during the lifetime of a particular calibration curve. For these reasons, the platform has been designed to be able to level and lock the drum in place. After correct placement of the drum on the platform, the load cell is calibrated by use of a balance which is accurate to ±0.1 g (±2.2e-5 lb_m).

While running the humidifier, the platform vibrated due to the motion of the boiling water. This fluctuation causes the measured evaporation curve to appear oscillatory. To alleviate this problem, we viewed the load cell output signal on an oscilloscope to determine the frequency of the oscillation. The signal noise clearly appeared to be a 2 Hz waveform. We filtered this signal with a 1 Hz low-pass filter to be sure of fully removing the noise from the signal. This action greatly improved the linearity of our evaporation data over the full range of the load cell measurement capability. Evidence of the linearity of our evaporation rate can be seen in Figure 2.10, which shows the weight change measured by the load cell with a 6 kW humidifier heat input. We plotted curves such as this for heat inputs of 2, 4, 6 and 8 kW and subsequently curve fit each set of data with a linear least squares fit. The results of these curve fits showed that the RMS error between the data points and their respective curve fits is less than 1% for each set of data. This error, however, is the error in the direct weight measurement. The error in the slope of these curves which corresponds to the error in our evaporation rate is much smaller.

We plotted the slopes of the four weight change curves in Figure 2.11. This graph shows the linearity of our ability to measure evaporation rate over the full range of humidifier heat inputs. It can be seen in Figures 2.10 and 2.11 that our ability to accurately measure the moisture input into the indoor room is excellent, and that this contributes positively to our measurement of room air conditioner moisture removal.

2.1.4 Temperature Measurements

Inside the room, we have two combined temperature and relative humidity probes for measuring the air-space properties. Temperature is measured by a platinum RTD with an accuracy of ±0.3°C. The probes are housed in aspirated radiation shields for obtaining true air measurements. These shields, which surround the probe bodies, are made of a white thermoplastic material to reflect incident radiation that could affect the temperature measurement. Aspirating fans are attached to the shields with a piece of PVC piping, causing air to be drawn across the sensing elements. This results in high heat and moisture transfer to the sensors, and thus more accurate

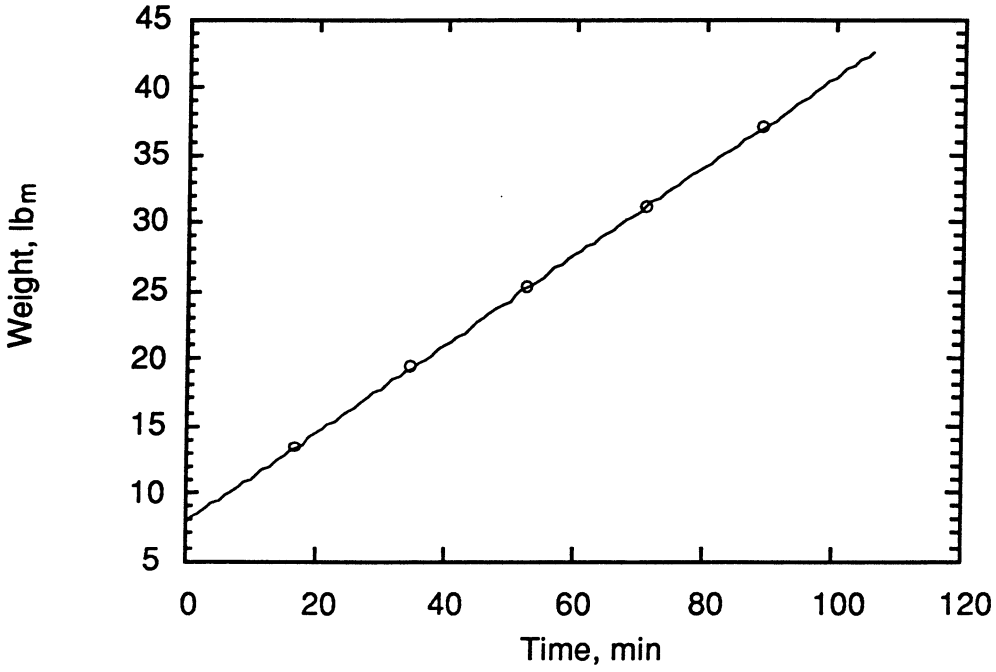

Figure 2.10 Measured Humidifier Weight Change with 6 kW Heat Input

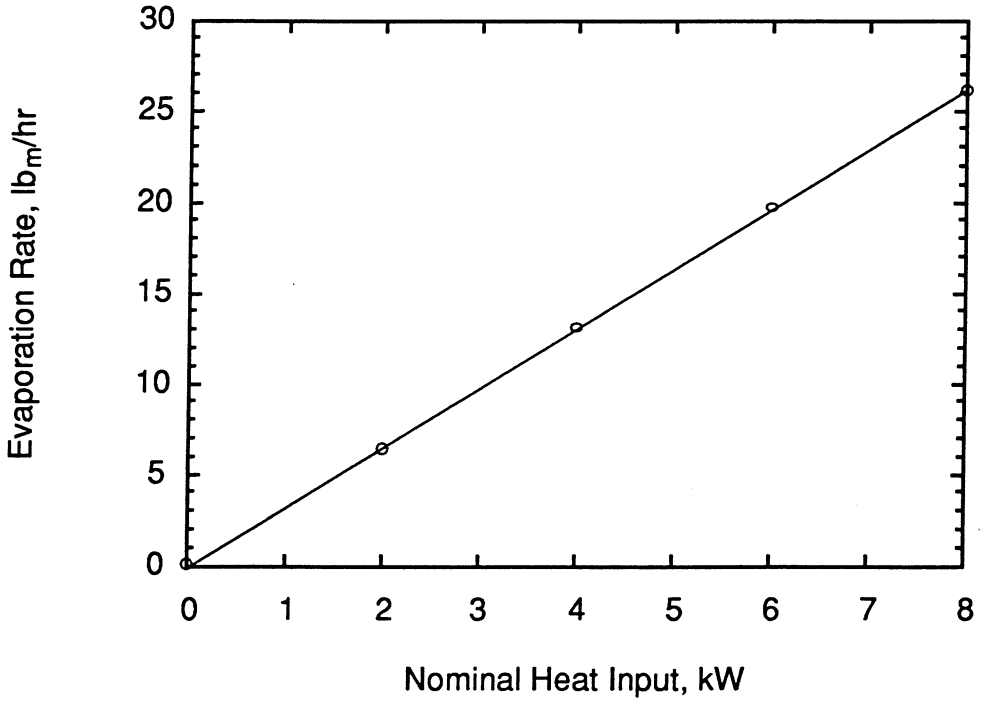

Figure 2.11 Measured Humidifier Evaporation Rate

measurement of air properties. These sensors will be used to control the temperature and relative humidity in the indoor room.

Also in the indoor room are twelve 30-gauge type-T thermocouples, which we use to measure wall temperatures for determining the mechanisms of heat transfer and the temperature distribution in the room. Although this thermocouple wire has a tolerance of 0.5°C, the accuracy of these measurements is of minor importance since we are using them to display trends in the room and not for exact temperature measurement. Four additional thermocouples are located in the guard space surrounding the calorimeter, and an immersion thermocouple is located inside the humidifier barrel to monitor the water temperature.

2.1.5 Humidity Measurements

As mentioned in the previous section, the relative humidity probes are located with the temperature probes in the indoor room. Relative humidity (RH) is measured by a capacitive-type humidity sensor with an accuracy of 2% in the range of 0 to 90% RH and 3% in the range of 90 to 100% RH. We set up an apparatus for calibrating these sensors over the range of 10% RH to 95% RH. This system utilized the relative humidity-temperature relationships between saturated-salt solutions in equilibrium with air (Wexler, 1954). This relative humidity-temperature relationship was recorded by Wexler and Hasegawa for several different salts over the range of 0 to 50° C. Our calibration setup utilized five of these salts (LiCl, NaCl, $Mg(NO_3)_2$, $MgCl_2$, and KNO_3) in order to cover the fullest range of relative humidity at room temperature.

The calibration apparatus consisted of a glass jar containing the saturated salt in solution with distilled water. This jar was outfitted with a special cap, on which were mounted two fittings. One of these was a screw-down compression fitting through which the sensor could be exposed to the known-humidity environment. This fitting tightened a rubber gasket around the sensor body so that no air leakage was permitted, and thus a constant humidity was maintained in the jar. The other fitting allowed for insertion of a thermocouple for reading the equilibration temperature in the jar. This port was also sealed to prevent air leakage.

Each sensor was tested in each of the five saturated-salt solutions. Comparison of the results predicted by Wexler and Hasegawa with those measured in each solution showed that the sensors were well within their claimed range of accuracy. In fact, most of the measurements, including a 93% RH condition, were within ±1.25% RH of the predicted values.

2.1.6 Data Acquisition

We use a Fluke 2280 datalogger to convert the signals from our sensors to values which can be stored or displayed. The datalogger has the capacity to measure 100 separate analog inputs at a maximum scan rate of 15 channels per second. This capacity is an important feature since we will need to make roughly 80 measurements throughout the test facility. The datalogger can read the RTD measurements to an accuracy of ±0.2°C and the thermocouples to an accuracy of ±0.65°C. DC Voltage measurements, such as the signal from the humidity sensors, can be read with a resolution of one part per hundred-thousand to an accuracy of 0.03% of the input signal. The capability of our datalogging system is not a limiting factor in the accuracy of any of our measurements. The datalogger is connected to a laptop personal computer, which remotely runs the datalogger's data acquisition program. The data is stored on a floppy disk and is converted to a spreadsheet format for data analysis.

2.2 Design of Outdoor Room

It should be noted that a more detailed description of the capabilities and performance of the outdoor room can be found in a document issued concurrently by Feller (1993). The following description is a brief overview of the system intended for continuity of the presentation.

The purpose of the outdoor room is to provide a chamber in which the room air conditioner condenser can be exposed to a uniform and steady-state temperature and humidity. A particular room air conditioner can reject both heat and moisture into the outdoor room. Most units are manufactured with a "sling ring", which consists of a cupped ring attached to the outer edge of the axial condenser fan blades. This ring allows the fan to lift condensate from the drain pan and throw it on the condenser, thus allowing it to evaporate. This feature allows the air conditioner to regain some of the energy lost condensing the moisture on the evaporator by using it to remove heat from the condenser. It also allows transfer of moisture from the indoor to the outdoor room. Since both heat and moisture are added to the outdoor room, reconditioning equipment is necessary for the removal of both of these quantities.

A 7-ton (25 kW) chiller provides both the heat and moisture removal necessary for operating the room at a wide variety of steady-state conditions. The chiller circulates a mixture of water and ethylene glycol through a fan-coil unit in the outdoor room. This unit uses a 1500 cfm blower to mix the air in the outdoor room as specified

by the ASHRAE standard. The chiller provides ±0.18 °F (±0.1 °C) temperature stability and a range of supply temperatures between 5 °F and 95 °F (-15 °C and 35 °C.) We can control the mass flow of water through the coil by use of a control valve mounted in parallel with the coil. By controlling the flow, heat transfer from the air to the coil is modulated to obtain a steady state temperature condition. Control of the chiller supply temperature, and thus the coil temperature, is used to maintain a constant dew point in the outdoor room.

2.3 Volumetric Airflow Measurement

Another parameter which is related to air conditioner performance is the volumetric airflow forced through each heat exchanger. We have designed a system to measure air volume flow over the full range of evaporator and condenser fan speeds. The system, shown in Figure 2.12, consists of a flexible air duct that is attached to the outlet of either heat exchanger. The flexible duct is made of a vinyl fabric which can be duct-taped around the edges of any room air conditioner heat exchanger to assure the capture of all airflow. The air conditioner blows air into the duct, through a piece of PVC piping, into a venturi meter, and then through another length of pipe. The venturi entrance and exit pipe lengths are sized to meet the manufacturers specifications for flow uniformity. The pressure drop imposed on the measured airflow by the venturi, duct and piping system is measured by an inclined manometer. Compensation for this pressure loss is achieved by controlling the speed of the make-up fan by using variable-frequency control of the fan motor. After equilibrating the system, volume flow is determined by reading the pressure drop across the venturi and measuring the temperature of the air (to calculate the air density).

The venturi itself measures flow within 1% of the actual flow. Inaccuracies involved in the system include errors due to reading analog pressure measurements. The operator decides when the system has come to equilibrium with the ambient by reading the manometer, which has gradations every one-hundredth of an inch of water. After deciding on the equilibrium point, the operator then reads a differential pressure gage, which has gradations every tenth of an inch of water.

This system has the capacity to measure airflow rates in the range of 400 to 1400 cfm by use of two venturis. A 4 in. mouth size venturi is used to measure flow in the range of 400 to 800 cfm, while a 6 in. venturi is used in the range 800 to 1400 cfm. There exists a tradeoff in the system between the size (and hence the readability of

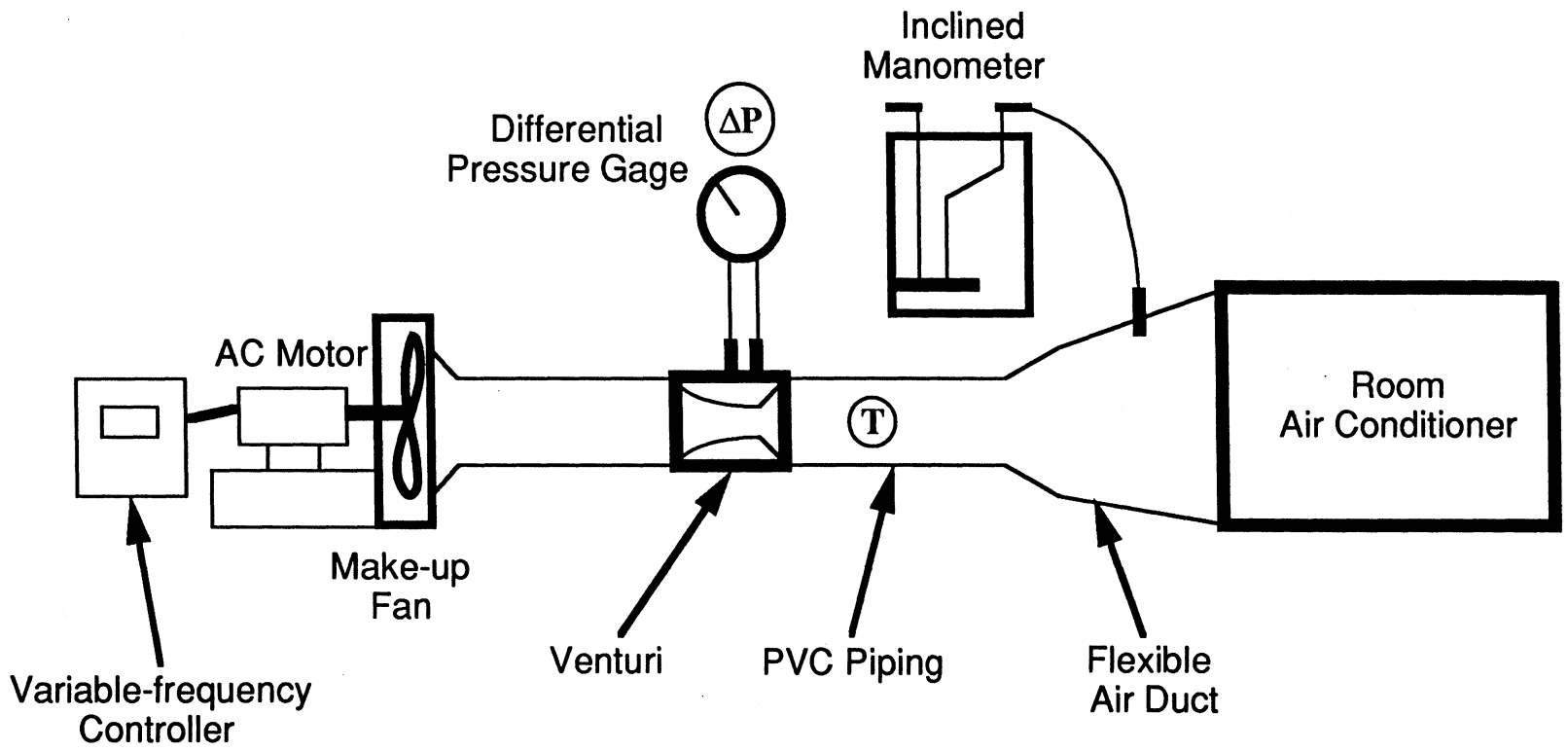

Figure 2.12 Volumetric Airflow Measurement System

the pressure drop across the venturi) and the permanent pressure drop imposed by the whole ducting system. As flow increases through the venturi, the permanent pressure drop increases as the square of the velocity. This phenomenon results in a very large load on the fan motor, which tries to compensate for the pressure loss. It also increases the measured pressure drop across the venturi, which increases the readability of the differential pressure measurement. The tradeoff between the high load on the fan motor and better readability creates the need to have venturis for two different ranges of flow.

3. OPERATING CHARACTERISTICS OF THE ROOM

A study of the steady-state and dynamic behavior of the indoor room was undertaken to determine the important performance characteristics and to identify any potential flaws in the design. Such data are essential for understanding and interpreting the energy and moisture balances and for laying out a schedule of future tests.

Before discussing the data, we shall describe a simple model of the indoor room which is useful for interpreting the results. Figure 3.1 illustrates how the energy and moisture balances are conceptualized. The major elements include (a) the air in the indoor room, (b) the walls of the indoor room, (c) the test unit, (d) the reconditioning equipment, (e) the air of the outdoor room and (f) the ambient. These last two elements give rise to the unavoidable parasitic losses. The "ambient", consisting of the total surroundings (including the outdoor room), is represented by a single area-weighted average temperature. The ambient is viewed as a large heat sink with which the walls may freely exchange heat. Because great care was taken to avoid moisture transfer to the walls of the room, there is no direct transfer of moisture to the walls. However, it is impossible to seal against moisture transfer through the passageways of the test unit itself. This exchange mechanism must be included in developing the moisture balance for the air in the indoor room.

The basic features of the model are summarized in Table 3.1. Here, the key assumptions are laid out, the governing equations are presented and their solutions are given. A simple lumped-parameter approach is used. The most important results of this analysis are as follows.

1. The model includes six parameters which characterize the exchange and storage mechanisms of the room, and one parameter f which characterizes the distribution of energy added by the reconditioning equipment. Using an electrical analogy, we may say that these first six parameters characterize the resistances and capacitances of the room. Specifically, the exchange mechanisms (resistances) are characterized by the three parameters $(U_1 A_1)$, $(U_2 A_2)$, and $(U_m A_m \rho_g)$; and the storage mechanisms (capacitances) are characterized by the three parameters $(m_a c_{pa})$, $(m_w c_{pw})$, and m_a.

2. At equilibrium, the energy removed by the test unit is equal to the energy added by the reconditioning equipment less a correction which accounts for the parasitic

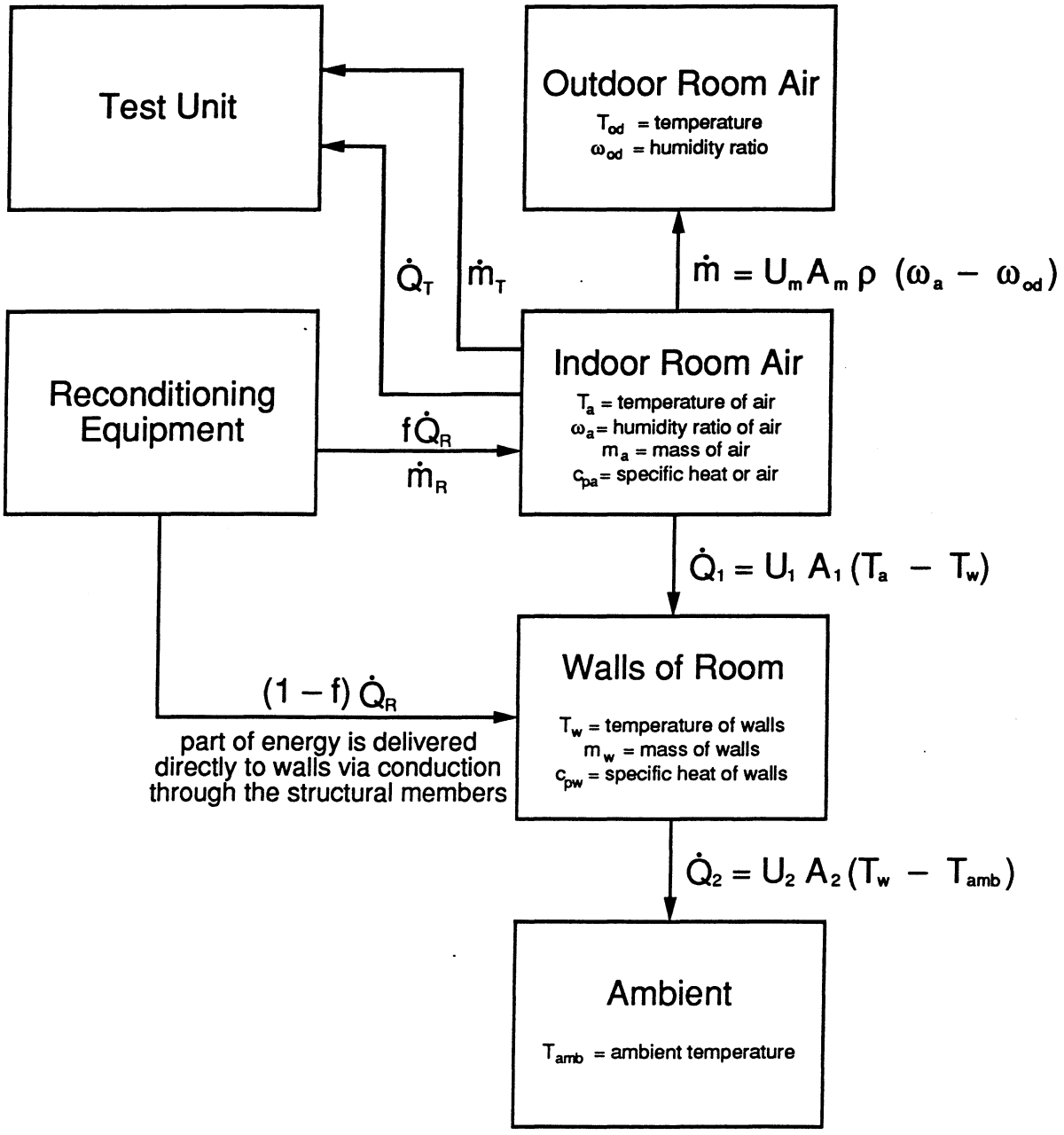

Figure 3.1 Schematic of Heat and Moisture Transfers to and from Indoor Room

Table 3.1 Summary of Simple Model for Indoor-Room Calorimeter

Basic Assumptions

1. The air in the indoor room can be represented by a single average temperature T_a and humidty ratio ω_a. The air is of mass m_a and effective specific heat c_{pa}.

2. The walls of room can also be represented by a single average temperature T_w. The walls are assumed to be completely sealed against moisture transfer. This latter assumption was validated by experimental data. The walls are of mass m_w and effective specific heat c_{pw}.

3. The test unit removes thermal energy and moisture from the air in the indoor room.

4. The reconditioning equipment supplies thermal energy and moisture at rates $\dot{Q}_R$ and $\dot{m}_R$, respectively. Fraction (1 – f) of the thermal energy output of the reconditioning equipment is transferred directly to the walls by conduction through the structural members. The remaining fraction (f) is transferred to the air. The entire moisture output of the reconditioning equipment is delivered to the air in the indoor room.

5. The air of the room and the walls of the room exchange heat at rate $\dot{Q}_1$ given by $U_1 A_1 (T_a - T_w)$, where U_1 is an overall heat transfer coefficient and A_1 is contact area.

6. The walls of the room exchange heat with the ambient. The ambient consists of the entire thermal surroundings of the indoor room including the outdoor room. The ambient is characterized by a single area-weighted average temperature T_{amb}. The rate of heat exchange $\dot{Q}_2$ is given by $U_2 A_2 (T_w - T_{amb})$, where U_2 is an overall heat transfer coefficient and A_2 is contact area.

7. The air in the indoor room exchanges moisture with the outdoor room owing the passages through the air conditioner in the partition wall. The rate of moisture transfer is $U_m A_m \rho_g (\omega_a - \omega_{od})$, where U_m is an effective mass transfer coefficient, A_m is an effective mass transfer area, ρ_g is air density, and ω_{od} is the average humidity ratio for the outdoor room.

Governing Equations

Energy Balance for Room Air:

$$\frac{d}{dt}(m_a c_{pa} T_a) = -U_1 A_1 (T_a - T_w) + f \dot{Q}_R - \dot{Q}_T \qquad (3.1)$$

Energy Balance for Walls:

$$\frac{d}{dt}(m_w c_{pw} T_w) = U_1 A_1 (T_a - T_w) - U_2 A_2 (T_w - T_{amb}) + (1 - f) \dot{Q}_R \qquad (3.2)$$

Moisture Balance for Room Air:

$$\frac{d}{dt}(m_a \omega_a) = -U_m A_m \rho_g (\omega_a - \omega_{od}) + \dot{m}_R - \dot{m}_T \qquad (3.3)$$

Table 3.1 Summary of Simple Model for Indoor-Room Calorimeter (continued)

The system is characterized in terms of seven basic parameters: (i) $U_1 A_1$, (ii) $U_2 A_2$, (iii) $U_m A_m \rho_g$, (iv) $m_a \omega_a$, (v) $m_a c_{pa}$, (vi) $m_w c_{pw}$, and (vii) f.

Initial Conditions

$$T_a(0) = T_{ao} \qquad T_w(0) = T_{wo} \qquad \omega_a(0) = \omega_{ao} \tag{3.4}$$

Steady-state Results

$$T_{a\infty} = T_{w\infty} + \frac{f\dot{Q}_R - \dot{Q}_T}{U_1 A_1} \tag{3.5}$$

$$T_{w\infty} = T_{amb} + \frac{\dot{Q}_R - \dot{Q}_T}{U_2 A_2} \tag{3.6}$$

$$\omega_{a\infty} = \omega_{od} + \frac{\dot{m}_R - \dot{m}_T}{U_m A_m \rho_g} \tag{3.7}$$

Expressing the energy and moisture removal rates of the test unit in terms of the steady-state, indoor-room conditions, we have

$$\dot{Q}_T = \dot{Q}_R - U_2 A_2 (T_{w\infty} - T_{amb}) \tag{3.8}$$

$$= \frac{g+f}{g+1}\dot{Q}_R - UA (T_{a\infty} - T_{amb}) \tag{3.9}$$

$$\dot{m}_T = \dot{m}_R - U_m A_m \rho_g (\omega_{a\infty} - \omega_{od}) \tag{3.10}$$

where $g = \frac{U_1 A_1}{U_2 A_2}$ and $UA = \frac{(U_1 A_1)(U_2 A_2)}{U_1 A_1 + U_2 A_2}$.

Using these results, (3.1) and (3.2) can be expressed as

$$\frac{d}{dt}\Delta T_a = \Delta T_w \alpha_1 - \Delta T_a \alpha_1 \tag{3.11}$$

$$\frac{d}{dt}\Delta T_w = -\Delta T_w \alpha_2 + \Delta T_a \alpha_3 \tag{3.12}$$

where

$$\Delta T_a = T_a - T_{a\infty} \tag{3.13}$$

$$\Delta T_w = T_w - T_{w\infty} \tag{3.14}$$

$$\Delta \omega_a = \omega_a - \omega_{a\infty} \tag{3.15}$$

Table 3.1 Summary of Simple Model for Indoor-Room Calorimeter (continued)

$$\alpha_1 = \frac{U_1 A_1}{m_a c_{pa}} \tag{3.16}$$

$$\alpha_2 = \frac{U_1 A_1 + U_2 A_2}{m_w c_{pw}} \tag{3.17}$$

$$\alpha_3 = \frac{U_1 A_1}{m_w c_{pw}} \tag{3.18}$$

Transient Results (assuming constant $\dot{Q}_T$ and $\dot{Q}_R$)

$$\Delta T_a(t) = - c_1 \exp(-\lambda_1 t) + c_2 \exp(-\lambda_2 t) \tag{3.19}$$

$$\Delta T_w(t) = c_3 \exp(-\lambda_1 t) - c_4 \exp(-\lambda_2 t) \tag{3.20}$$

and

$$\Delta \omega_a(t) = \Delta \omega_{ao} \exp(-\lambda_3 t) \tag{3.21}$$

where

$$\lambda_1 = b + \sqrt{b^2 - c} \tag{3.22}$$

$$\lambda_2 = b - \sqrt{b^2 - c} \tag{3.23}$$

$$\lambda_3 = \frac{U_m A_m \rho_g}{m_a} \tag{3.24}$$

$$b = \frac{1}{2}(\alpha_1 + \alpha_2) \tag{3.25}$$

$$c = \alpha_1(\alpha_2 - \alpha_3) \tag{3.26}$$

$$c_1 = \frac{\Delta T_{wo}\alpha_1 + \Delta T_{ao}(\lambda_2 - \alpha_1)}{\lambda_1 - \lambda_2} \tag{3.27}$$

$$c_2 = \frac{\Delta T_{wo}\alpha_1 + \Delta T_{ao}(\lambda_1 - \alpha_1)}{\lambda_1 - \lambda_2} \tag{3.28}$$

$$c_3 = \frac{\Delta T_{wo}(\lambda_1 - \alpha_1) - \Delta T_{ao}\alpha_3}{\lambda_1 - \lambda_2} \tag{3.29}$$

$$c_4 = \frac{\Delta T_{wo}(\lambda_2 - \alpha_1) - \Delta T_{ao}\alpha_3}{\lambda_1 - \lambda_2} \tag{3.30}$$

loss through the walls to the ambient. This parasitic loss is a well-defined function of the temperature difference between the air in the room and the ambient temperature.

3. Similarly, the moisture removed by the test unit equals the moisture added by the reconditioning equipment less a correction which accounts for the parasitic loss to the outdoor room. This correction is a well-defined function of the difference in humidity ratio between the indoor and outdoor rooms.

4. The transient response of the system is characterized by two time constants ($1/\lambda_1$ and $1/\lambda_2$). We shall refer to these as the "long" and "short" time constants, respectively. The long time constant determines how quickly the system reaches steady state.

5. Two parameters, m_a and $m_a c_{pa}$, can be determined from geometric considerations alone since only the air inside the room need be considered. The remaining parameters, although physically meaningful, must be determined empirically by analyzing the steady-state and transient behavior of the room.

6. The parameters of greatest practical interest are (i) the UA-value for parasitic heat loss from the room at steady state, (ii) the $UA\rho_g$-value for parasitic moisture loss from the room at steady state, and (iii) the two time constants governing transient behavior. The following discussion will focus primarily on these three sets of parameters.

3.1 Test Facility Behavior without Room Air Conditioner Running

The first tests performed in the facility were run without the air conditioner operating. These were used to determine the system behavior at both steady-state and dynamic conditions. These tests are critical to the complete evaluation of the facility because the data obtained is independent of the air conditioner, and is thus more representative of the calorimeter itself.

3.1.1 Heat Loss Tests

Heat loss from the indoor room can be most easily measured by maintaining the room at a constant temperature with a precisely known heat input. At steady-state, the

heat input equals the heat leakage through the walls. Such testing must be performed without the air conditioner and reconditioning equipment running, since the energy transfer associated with these devices easily overwhelms the losses being measured. In fact, the fans of reconditioning equipment alone dissipate more energy than is lost through the walls of the room over the range of temperature differences of interest to us. Fortunately, the conduction resistance of the walls is more than 8500 times the convection resistance between the air and the walls, so that the slight difference in convection resistance between the stagnant room and the mixed room is negligibly small indeed.

The heat exchange through the walls of the chamber was first measured with the air conditioner window plugged with insulation of the same type and thickness as the walls. A 100-W light bulb supplied the heat load for the indoor room. The voltage applied to the light bulb was controlled by an autotransformer so that the heat input could be regulated. We selected four levels of heat input at which to gather data. After the room reached a steady-state temperature at each heat input level, we measured the power drawn by the light bulb and recorded the indoor and outdoor room temperatures. Heat loss is plotted versus the temperature difference between the indoor and outdoor rooms in Figure 3.2. Here, we assume that the air spaces surrounding the chamber were at the same temperature as the outdoor room. This assumption produces some error in the heat loss calibration, but reasonable results are nevertheless obtained for the overall heat transfer resistance of the walls. The resistance calculated from a linear least-squares curve fit of the data in Figure 3.2 corresponds to an R-value of 77. This result compares favorably with the R-value of 84 calculated based on the quoted conductive resistance of the foam. Another small, but unavoidable source of error in the calibration is the temperature gradient in the room. Some care is necessary in placing the sensors. This point is especially important when a test unit is present as is more fully addressed below.

A second test was performed with a Whirlpool 1.5-ton air conditioner mounted in the partition wall. In this case, individual temperatures were measured at several locations in the air space surrounding the indoor room, allowing for a more representative ambient temperature to be calculated. Moreover, since we have some experience operating this particular air conditioner, we also have a good idea where to measure the average room temperature to minimize the effect of gradients.

The area-weighted-average ambient temperature is computed using the following relationship.

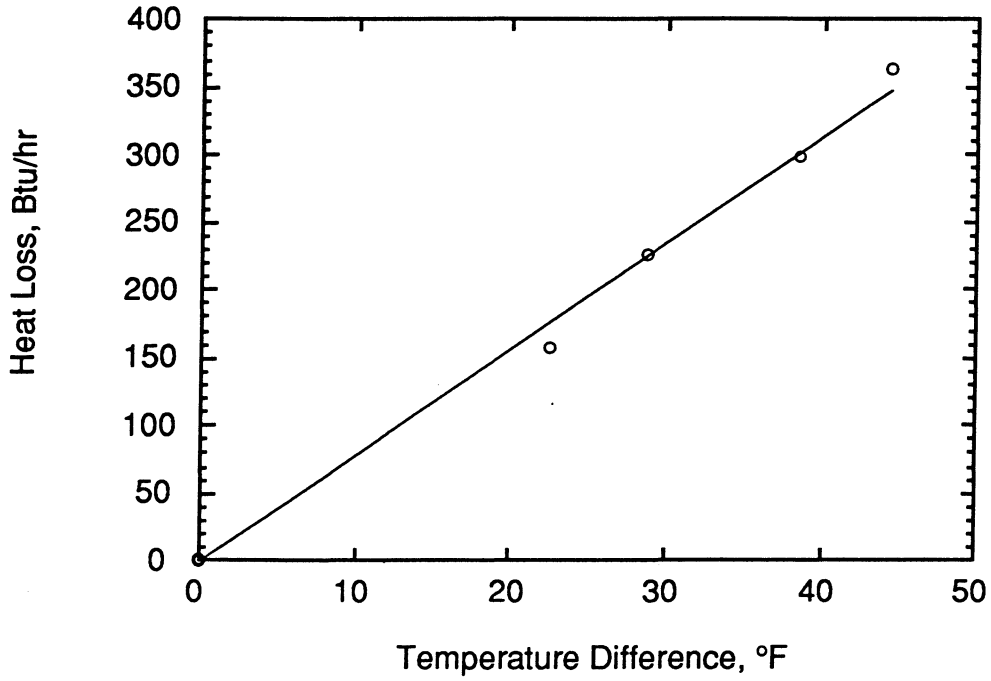

Figure 3.2 Heat Loss with Plugged Wall

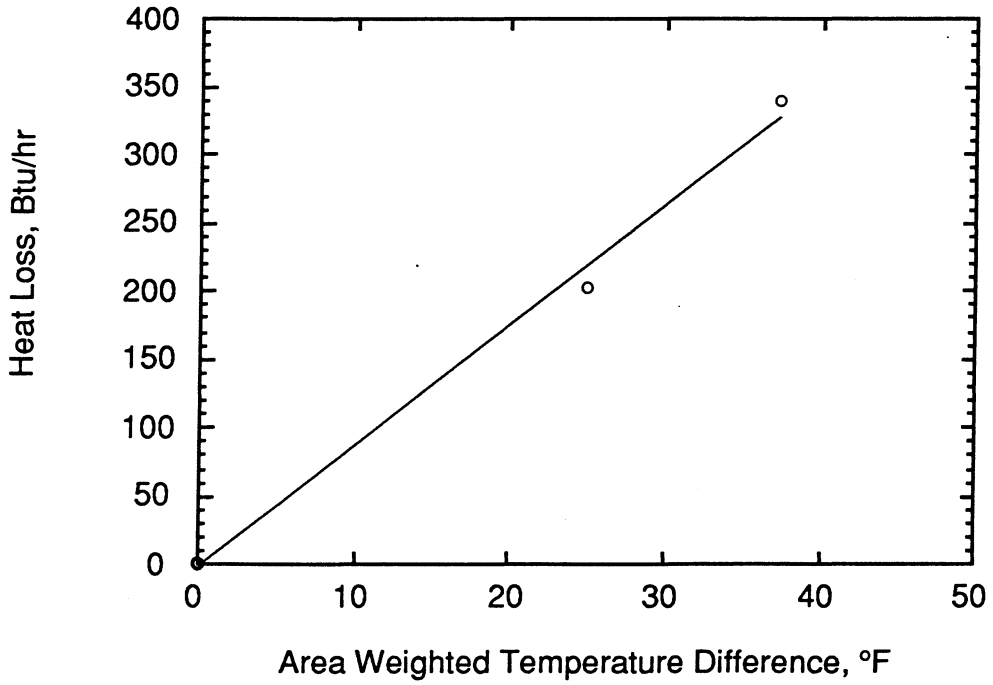

Figure 3.3 Heat Loss with Air Conditioner in Wall

$$\overline{T} = \frac{1}{A} \sum_{i=1}^{6} A_i T_i \ , \qquad (3.23)$$

where T_i represents each of the six temperatures measured in the space surrounding the room (one of which is the outdoor room temperature) and A_i is the effective wall area associated with that temperature. A UA-value can then be determined from the difference between this average ambient temperature and the average room temperature T_a using the following relationship.

$$UA = \frac{\dot{Q}}{Ta - \overline{T}} \ , \qquad (3.24)$$

where $\dot{Q}$ is the energy added to the room.

The results of this test are shown in Figure 3.3. The slope of the best-fit line corresponds to a UA value of roughly 8.8 Btu/hr-°F. For the plugged wall case discussed above, a value of 7.9 Btu/hr-°F was found. These results show that roughly 10% of the total heat loss is due to the presence of the test unit . Since the heat transfer area associated with the air conditioner is less than 1% of the total wall area, we conclude that the local heat flux through the air conditioner is at least 10 times greater than the heat flux through the walls of the chamber.

Figure 3.3 provides a calibration curve by which to adjust our air-side energy balance on the room. The uncertainty in the calibrated heat loss is less than 10%. Assuming a 50 °F temperature difference, the predicted heat loss is 450 Btu/hr with an uncertainty of less than 45 Btu/hr. The maximum uncertainty in our energy balance is thus on the order of 0.75%, even for our smallest test unit with a capacity of 6000 Btu/hr.

It is important to note that a calibration of this type is necessary for each unit tested to account for differences in heat loss characteristics. Moreover, the calibration is most accurate if the temperature sensors are placed at the same location in the room for all tests conducted with a particular unit.

3.1.2 Moisture Loss Tests

As noted previously, the room was carefully constructed to eliminate moisture transfer to the walls of the room. Unfortunately, it not possible to eliminate moisture transfer through the passageways of the test unit. Consequently, we must determine this rate in order to properly correct the overall moisture balance for the room. The parasitic moisture transfer rate can be correlated with the difference in humidity ratio

between the indoor and outdoor rooms following a procedure parallel to that used for the steady-state heat loss.

Because the transfer rate is so small, we are unable to measure it directly using a steady-state test of the type described above for heat transfer. Instead, we conducted a transient test and then used our simple model along with the directly computable mass of air in the room to determine the transfer coefficient. The test was carried out by raising the indoor room to a high humidity and observing how the humidity approaches the value of the outdoor room over time.

Figure 3.4 shows the results of a test conducted with the Whirlpool 1.5-ton unit in place but not running. In a matter of a few minutes, the humidifier raised the moisture content of the air from 0.005 to 0.025 lb_m-H_2O/lb_m-dry-air. Initially, the humidity ratio seems erratic. We attribute this behavior to inhomogeneities in the moisture concentration due to the lack of active mixing in the room. After this initial period, the humidity ratio declined exponentially over the 70-hr logging period. The time constant for this decay is 86 hr. Based on an air mass of 45 lb_m, we determine that $U_m A_m \rho$ is 0.52 lb_m-air/hr. This value is multiplied by the humidity ratio difference to determine the correction for the moisture balance. For example, a high humidity ratio difference of 0.02 lb_m-H_2O/lb_m-air gives a correction of only about 0.01 lb_m-H_2O/hr. This value is quite small compared with the moisture removal rate under most operating conditions. Figure 3.4 also shows that the outdoor room humidity ratio varies considerably around an average value. Because the outdoor room was left open during this test, the measured humidity ratio is just that of the surrounding laboratory.

We experimented with the moisture dynamics of the indoor room to determine the response of the system to changes in moisture input and removal rates. Results of this study show that moisture can be quickly added to and removed from the indoor room air, which suggests a minimal moisture capacitance in the room. The moisture removal test is included in this section, even though it requires the operation of the air conditioner.

The response of the humidification system at operating temperatures is very quick. One can change the evaporation rate from the maximum value of 27 lb_m-H_2O/hr to nearly zero instantaneously. However, bringing the nearly 100 lb_m of water in the drum up to operating temperature can take 45 minutes to an hour depending on the initial condition. After the system has been raised to operating temperature, response to a step change in moisture demand is rapid.

To test the moisture removal, an additional test was performed after the one described in Figure 3.4. After the moisture level in the indoor room was allowed to

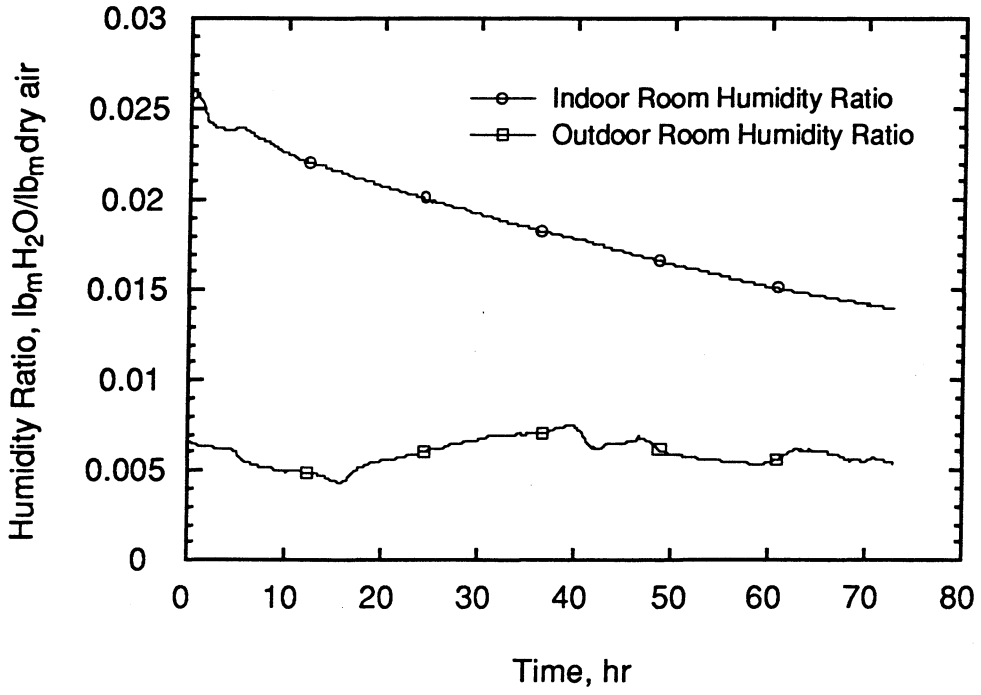

Figure 3.4 Response of Indoor Room to Initial Humidification

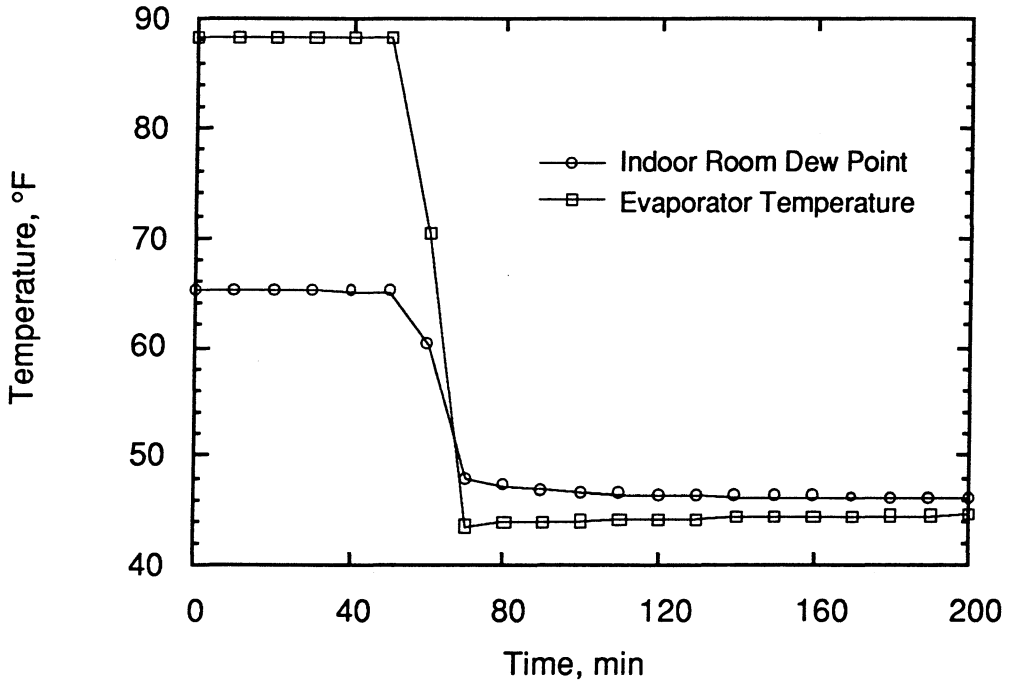

Figure 3.5 Response of Moist Indoor Room to Sudden Air Conditioner Operation

decay, we turned the air conditioner on to dehumidify the room and added heat with the furnace so that the evaporator coil would not frost. The effect of this action on the indoor room dew-point temperature is shown in Figure 3.5. The test unit pulled the dew-point temperature down by 17 °F (0.006 lb_m-H_2O/lb_m-dry-air) to a new level over a 20 min period. Figure 3.5 also shows how the new steady dew-point temperature is controlled by the evaporator coil temperature. The moisture removal rate corresponding to this change was approximately 1 lb_m-H_2O/hr. From these data, it can be seen that a change from a high steady moisture level condition to lower steady moisture level is also a rapid process. Consequently, we conclude that the moisture capacitance of the system is small.

We logged the weight reading from the humidifier throughout the duration of the test. Although no evaporation was occurring, we noted that the amplified and filtered output of the load cell was oscillating. We determined that this oscillation followed a diurnal cycle matching the periodic variations of the building voltage. The output signal oscillated for one of two reasons. Either the load-cell excitation voltage supplied by the DC power source is dependent upon the building voltage, or the gain of the amplifier in the low-pass filter is affected by this voltage variation. In future work, measures will be taken to assure that steady power is supplied to the load cell and that the output is steadily amplified.

3.2 Test Facility Behavior with Room Air Conditioner Running

We operated the test facility with the air conditioner and furnace running in order to identify the behavior of the test chamber while approaching, and after having reached, a steady-state temperature. We set the furnace controller to give a constant heat input to the room and ran the air conditioner until a steady temperature was reached. These tests simulated the full operation of the facility, with the exception that the humidifier was not used.

3.2.1 Sensible Heat Addition Only

We ran approximately fifteen of these steady-state tests, keeping the temperature of the outdoor room constant and varying the heat input to the indoor room. The behavior we observed is sharply influenced by the short time constant of the room, which we determined to be 2 hr. Somewhat less apparent but equally important is the long time constant, which we determined to be 9.5 hr. The long time constant is important in developing a series of tests for each unit, because we wish to be close to

steady state so that the correction in the energy balance is small. It may well be that we will elect to use a transient correction as well as a steady state correction in order to reduce the waiting time between data points.

Figure 3.6 shows the temperature response due to heating at what we believed was a constant level. The problem we discovered while running this series of tests was that the indoor room temperature varied around a quasi-steady state and never settled to a single value. As can be seen in Figure 3.6, the main peaks of the temperature curve occur at 24-hr intervals. These data, in conjunction with subsequent runs during which voltage was logged, confirmed that the oscillations are indeed on a diurnal cycle, and that they are directly traceable to the temporal variation in the building voltage. Since the duty cycle of the heaters is fixed, changes in voltage produce corresponding changes in heat input. Two alternatives for eliminating this problem are immediately obvious. One involves regulating the voltage; the other involves the use of feedback control to maintain a constant power input. Future work will involve either one or both of these modifications.

Because of the long time constant, the indoor room temperature moves toward equilibrium very slowly. We found that as the room approaches equilibrium, the change in temperature is less than 1 °F/hr even though the temperature itself is still several degrees from equilibrium. The ASHRAE Standard uses a rate constant of less than 1 °F/hr for room temperature as the criterion for defining a steady-state operating condition in the indoor room. We see that it is important not to confuse the approach to equilibrium with actual equilibrium, since a non-equilibrium condition will cause a significant error in the indoor room heat balance unless an unsteady correction is applied.

We also investigated the temperature stratification in the indoor room to check the uniformity of the air temperatures, especially near the evaporator entrance. The evaporator inlet temperature is the temperature of greatest interest in this study. Ideally, we desire the indoor room temperature to be uniform at the evaporator inlet temperature. However, we quickly realized that stratification always exists to some degree in front of the air conditioner when it is operating. The unit causes this stratification itself, and thus it cannot, and indeed should not, be eliminated. With the present test unit, depending upon sensor placement, temperature readings taken in a vertical plane two feet in front of the face of the air conditioner can differ by as much as 15 °F. Such large differences make it difficult to measure a value which is representative of the inlet temperature. Because stratification is different for every air

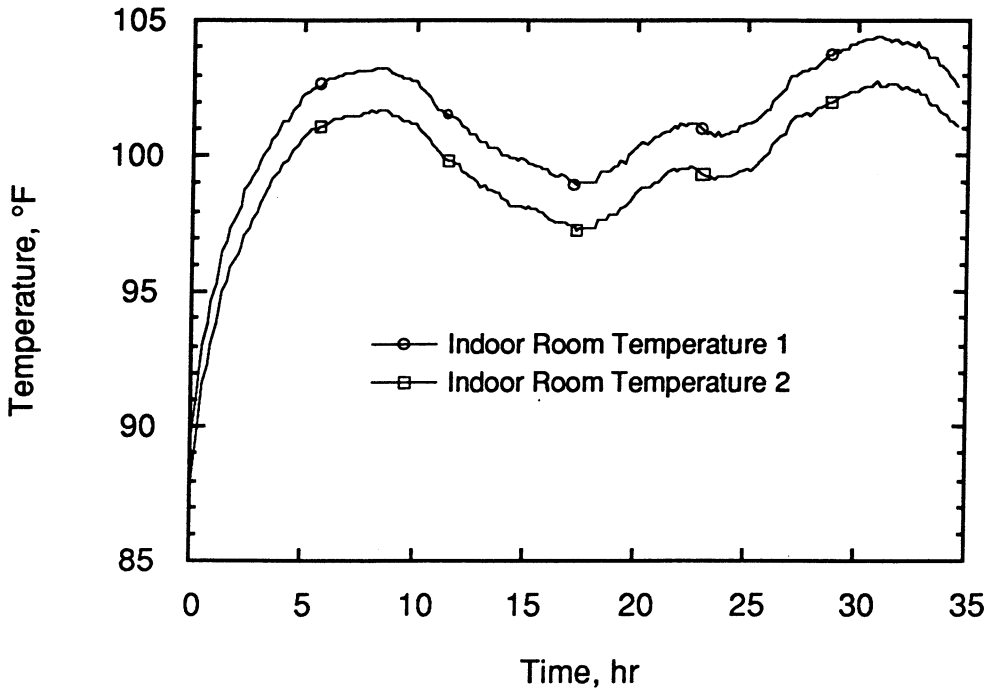

Figure 3.6 Transient Response of Indoor Room

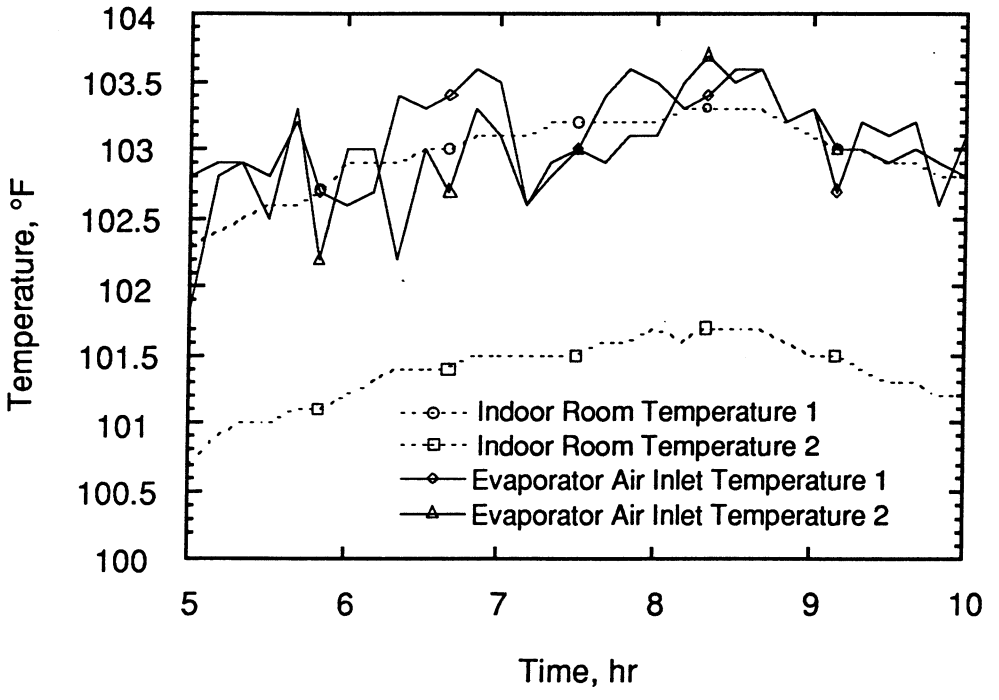

Figure 3.7 Indoor Room Air Temperatures at Quasi-steady-state

conditioner, sensor placement must be individually determined based on experience with that particular unit.

For the Whirlpool 1.5-ton unit, we selected two sensing positions geometrically centered at the edges of the air conditioner face in the vertical plane 2 ft in front of the air conditioner face. Figure 3.7 shows the indoor room temperatures sensed by the RTD's. The air conditioner, in concert with the furnace, produces temperatures at these positions which fall within a 1.5 °F band. However, this effect is due to the fact that the air conditioner blows more air out in the direction of the cooler sensor. Perhaps a less geometric means of measuring temperature would yield closer results.

Figure 3.7 shows these two indoor room temperatures as related to the temperatures at the evaporator inlet. We measured the inlet evaporator temperature with two thermocouples centered on the grille of the air conditioner. As is shown in Figure 3.7, these temperatures vary considerably but keep the same mean which tracks the first indoor room temperature reading. The RTD's read a much more constant temperature since they are shielded and draw in a better mixed air sample. Ideally, we would like to measure and control the air temperature with the signal from the RTD's (as positioned above) and be confident that the measurement is representative of evaporator inlet and average room air temperatures. This requires some experimentation with the placement of the cooler reading sensor in order that it be moved totally out of the flow of the evaporator. One cannot guarantee that temperatures will always agree for any single test unit, but it is certainly within our means to adjust airflow or sensor placement in the room in order to read good average room temperatures that are indicative of evaporator inlet temperatures.

3.2.2 Sensible and Latent Heat Addition

We can assess the time constant of the moisture addition process by running the indoor room at a set heat and moisture input and then introducing a step change in moisture input. Though the heating process is slow, the moisture addition process is believed to be rapid between steady-state conditions . The time required for testing is reduced if we hold the temperature of the system constant and change only the humidity level.

With the air conditioner running, a set heat input into the room and the humidifier at operating temperature, we added moisture to the room at a rate of 3.6 lb_m-H_2O/hr. The system response is shown in Figure 3.8. Within an hour, the humidity level in the room became fairly steady. It did not reach a total steady-state because the

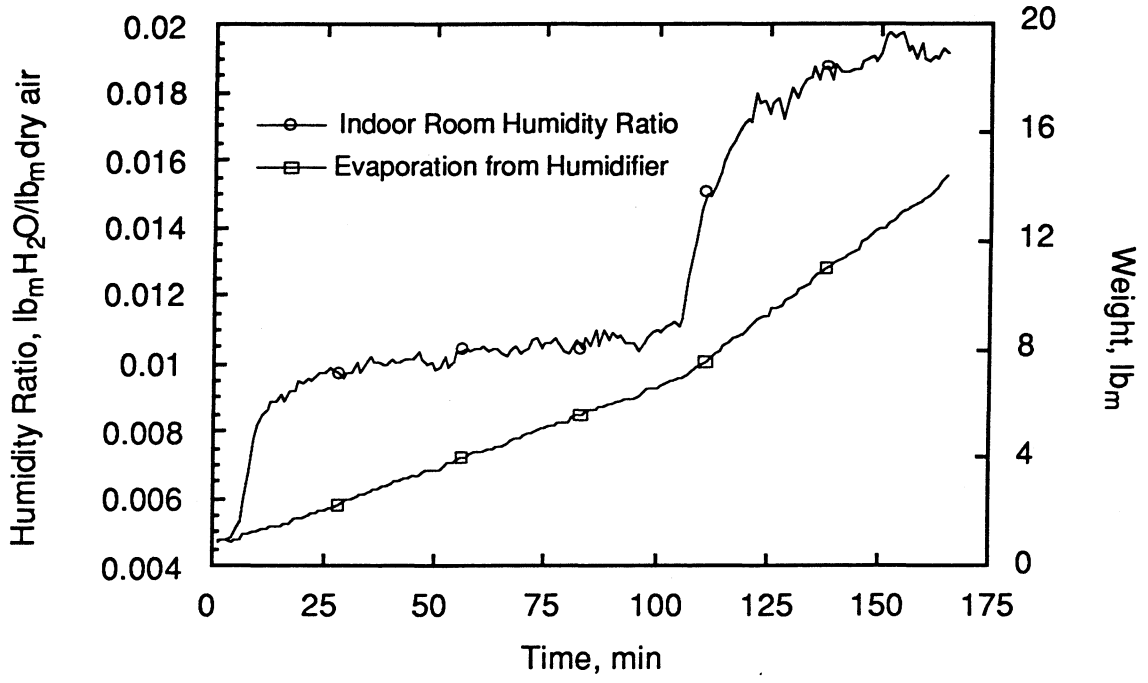

Figure 3.8 Humidity Response of Indoor Room to Change in Evaporation Rate

temperature in the room is rising, which is causing the operating condition of the air conditioner to change. Figure 3.8 also shows the weight change of the humidifier. At a time of 110 min, the evaporation rate is doubled to 7.2 lb_m-H_2O/hr as shown by the change in slope of the evaporation curve. The humidity ratio again seems to reach a quasi-steady state in about 1 hr. This phenomenon indicates that we are correct in believing that the system responds much more quickly to moisture addition than to heat addition.

As of yet, we don't have as much experience running the room with heat and moisture inputs as we do running it with only a heat input. Since the time constant due to heating is much greater than that due to moisture addition, the time constant of heating drives the response of the system. So far, the only peculiarity we have noticed in our data during steady-state testing is a variation in the dew-point temperatures that our sensors read. This fluctuation over a 3 °F range was not evident in our heat addition data sets. It is possible that the sensors are placed too close to the outlet of the humidifier and that the moisture is not well mixed within the air. Further experimentation is necessary to determine the cause of the problem and find a remedy.

By analysis of the data acquired on the performance of the indoor room, we have quantified the parameters which characterize system operation. These are shown in Table 3.2.

3.2.3 Volumetric Airflow Results

Although it does not directly relate to the study of the indoor room, knowing the evaporator and condenser air flow rates is important for modeling air conditioner operation. Because accurate measurement of air flow rates *in situ* is virtually impossible, we elected to measure the air flow rate prior to unit installation using a simpler and far more accurate method. Because flow rate may depend on inlet temperature, we set up heaters at the air inlets of the heat exchangers. Specifically, we ran the volumetric airflow measurement system over a range of 45 to 70 °F for the evaporator and 70 to 95 °F for the condenser in order to determine the temperature effect. Results of these tests are shown in Figures 3.9 and 3.10. From these figures, one may readily observe that the trends in the data are quite linear for all fan speeds. Assumption of a constant volumetric flow rate based on inlet temperature is reasonable.

Table 3.2 Indoor Room Operating Parameters

Operating Parameters	
Parameter	Value
m_a	45 lb_m
$m_a c_{pa}$	10.8 Btu/°F
$m_w c_{pw}$	16.9 Btu/°F
$U_1 A_1$	1.4 Btu/hr-°F
$U_2 A_2$	6.6 Btu/hr-°F
$U_m A_m \rho g$	0.52 lb_m-air/hr
$1/\lambda_1$	2 hr
$1/\lambda_2$	10 hr

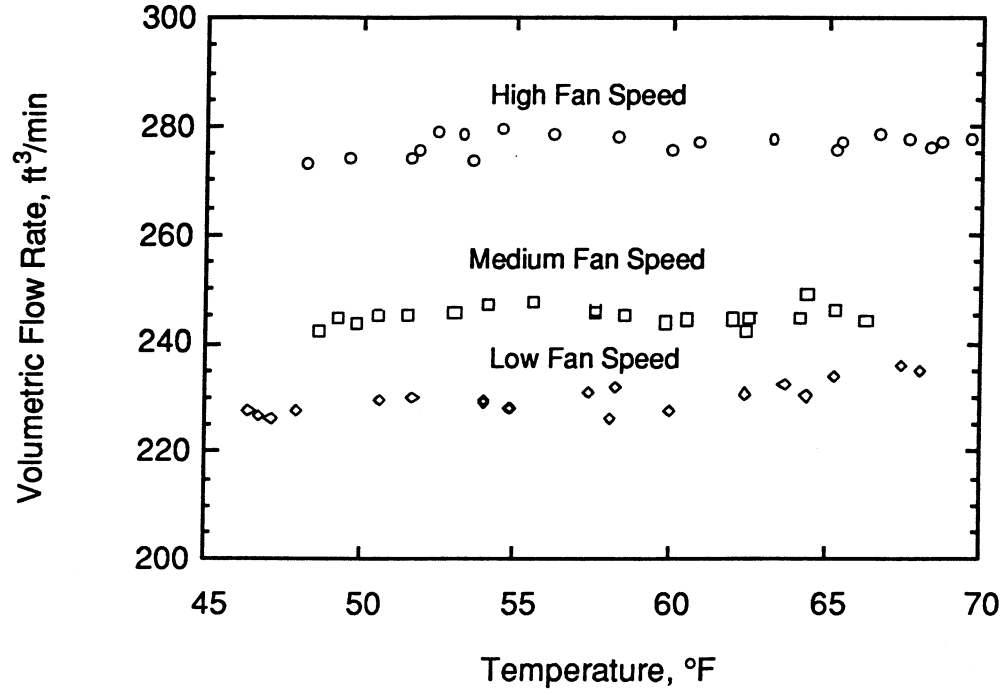

Figure 3.9 Evaporator Volumetric Airflow for Whirlpool 1 Ton Test Unit

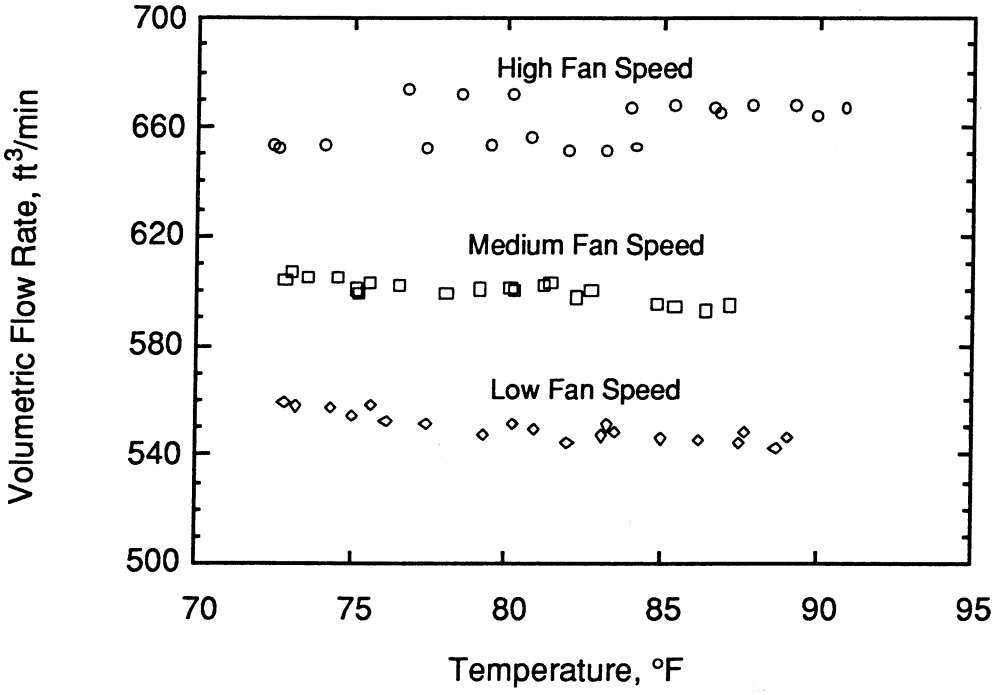

Figure 3.10 Condenser Volumetric Airflow for Whirlpool 1 Ton Test Unit

4. SUMMARY AND CONCLUSIONS

Manufacturers of room air conditioners expend much time and effort testing and improving the energy efficiency of their product. The need to assess the performance of room air conditioners has intensified due to tightening government mandated energy-efficiency standards on household appliances as well as the introduction of new refrigerants triggered by the environmental impact of CFC's in the atmosphere. This thesis has been written as part of an ongoing effort aimed at determining the effects of refrigerant and design changes on system performance. The work accomplished here in the design and construction of a test facility is the first step in a continual process.

We have designed the test chamber to measure the cooling and dehumidifying abilities of room air conditioners rated between 0.5 and 2.5 tons of refrigeration. The indoor room of the chamber has been outfitted to provide an environment for testing air conditioners over a wide range of psychrometric conditions. This method allows for the acquisition of a rich set of data, which will provide a basis for determining the effects of alternative refrigerants and their associated design changes on system performance. These data will also facilitate the verification of a concurrently developed room air conditioner simulation model.

Our design borrows heavily from the calibrated room calorimeter specified by ASHRAE Standard 16-1983. However, we improved upon this concept by constructing the chamber with very heavily insulated walls. The walls permit a very small parasitic heat loss that we can calibrate and use to correct the overall heat balance needed to determine the energy removal rate of the air conditioner. The error in this energy balance, associated with heat loss, is simply the error involved in our prediction of heat loss. The maximum error is small even as a percentage of the smallest test unit capacity. The chamber has been sealed meticulously such that we have almost unmeasurable moisture leakage and storage rates. These rates introduce an error to our overall moisture balance which is on the same order as the error associated with the heat loss calibration.

The test facility has been constructed and all of the sub-systems associated with the indoor room have been verified to be performing to their specifications. The humidification system accurately measures the amount of moisture added to the indoor room to 0.05 lb_m. The error associated with predicting the moisture addition rate is also small. This system, in combination with an accurate power measurement

system and the quantified heat and moisture transfers through the indoor room, will provide the means by which we can make accurate performance measurements.

The dynamic response of the indoor room has been illustrated and time constants associated with the heat and moisture addition processes have been quantified. These results will aid the operator of the facility when planning a testing schedule. The limiting time constants in the system are associated with heating the indoor room. Heavy testing schedules will warrant the need for an advanced control scheme for optimizing the amount of time needed to bring the system to steady-state and then moving on the next steady-state condition. A method for over-relaxing the response of the system may prove beneficial in reducing the response time required to reach equilibrium.

We found that steady-state conditions were not easy to maintain in the indoor room given the fact that the fluctuations in building voltage were causing fluctuations in the heat input into the room. We must determine whether the specified closed-loop temperature control is feasible for controlling temperature. If so, temperature will be controlled to a constant level and the problems associated with fluctuations in heat input will be eliminated. If we decide that controlling the power input into the room is a better method of controlling temperature, we will need to regulate the power supplied to the heating elements.

REFERENCES

ASHRAE (1984). Method of Testing for Rating Room Air Conditioners and Packaged Terminal Air Conditioners. Atlanta, ASHRAE Publications.

ASHRAE (1993). "ASHRAE supports revised Montreal Protocol." ASHRAE Journal **35**(1): 6.

Feller, S. D. (1993). Design of the Outdoor Environmental Chamber of a Room Air Conditioner Test Facility. University of Illinois at Urbana-Champaign.

Gavin, P. M. (1983). A Theoretical and Experimental Investigation of Evaporation from Drops Containing Nonvolatile Solutes. University of Illinois at Urbana-Champaign.

Miro, C. R., J. E. Cox. (1993). "Refrigerant issues highlighted at Society meeting." ASHRAE Journal **35**(3): 14.

NAECA. (1987). National Appliance Energy Conservation Act of 1987. Public Law 100-12.

Squair, P. (1993). ARI testifies at public hearing on accelerated phaseout rule. Koldfax (ARI). **19:** 8.

United Nations Environmental Programme. (1987). Montreal protocol on substances that deplete the ozone layer. New York, United Nations.

Wexler, A., S. Hasegawa. (1954). "Relative Humidity-Temperature Relationships of Some Saturated Salt Solutions in the Temperature Range 0° to 50° C." Journal of Research of the National Bureau of Standards **53**(1): 19-26.